CREVICE CORROSION IN ALUMINUM ALLOYS

A THESIS

Presented to

The Faculty of the Division

of Graduate Studies

By

Leon C. Green, Jr.

In Partial Fulfillment

of the Requirements for the Degree

Master of Science in Metallurgy

Georgia Institute of Technology

June, 1976

CREVICE CORROSION IN ALUMINUM ALLOYS

Approved:

Chairman Miroslav Marek,

Robert F. Hochman

Edgar A. Starke, Jr.

Date Approved by Chairman: 5-18-76

ACKNOWLEDGMENTS

TABLE OF CONTENTS

Crevice Corrosion
Crevice Corrosion in Aluminum Alloys
Crevice Solution Chemistry
Analytical Methods

Sample Preparation
Electrochemical Measurements
Measurement of pH
Analysis for Metallic and Chloride Ions
Polarization Measurements

Visual Observations
pH Measurements
Electrochemical Measurements
Solution Chemistry
Polarization Measurements

Crevice Corrosion on Al-Mg-Zn-Cu Alloys
The Mechanisms of Crevice Corrosion
Crevice Solution Chemistry

LIST OF TABLES

LIST OF FIGURES

SUMMARY

Crevice corrosion of aluminum-zinc-magnesium-copper
alloys in a neutral, 3.5% sodium chloride solution was investi-
gated on three alloys containing various amounts of copper.
Electrode potentials and galvanic currents were measured
using an artificial crevice cell of single geometry. The
reaction in the crevice was analyzed and the changes in
acidity, chloride ion concentration, and metallic ion concen-
tration were determined as a function of time. The effects
of corrosion were observed visually and examined in an
optical microscope. Polarization behavior of the electrodes
in the sodium chloride solution was examined.

The results show that the addition of copper increases
the rate of corrosion. In the crevice cells an acceleration
of the corrosion rate was observed and related to the
changes in the crevice solution chemistry, especially
acidification due to the hydrolysis of aluminum ions. Pitting
and grain boundary attack were observed in the crevices.
The solution chemistry results have been compared with
calculations based on thermodynamical data.

CHAPTER I

INTRODUCTION

Pure aluminum is very resistant to general corrosion
because of its ability to easily passivate and form various
oxide films that effectively retard most forms of general
corrosion.[1,2] In all natural environments; rural, marine,
or industrial, aluminum oxidizes very rapidly, and in case
of surface damage will repair its oxide layer before extensive
corrosion can occur. This film is stable over a wide pH
range, although strong acids and alkalis can dissolve the
protective film and leave the surface open to both uniform
and localized corrosion.[3,4] Despite the excellent corrosion
resistance, very little pure aluminum is used for commercial
or industrial purposes because of its low strength. Industrial
aluminum is usually alloyed with various elements, such as
copper, magnesium, zinc, and silicon to improve its overall
characteristics.[5,6] The common types of alloys and their
designations are listed in Table 1.

The alloying of aluminum, however, tends to decrease
its corrosion resistance. This susceptibility to corrosion
of the aluminum alloys depends upon the type and amount of
alloying elements, and the environment.[4] Of all the
alloying species, copper has the greatest effect of decreasing

Table 1. Aluminum Alloys

Series	Alloying Elements
1XXX	Pure Aluminum
2XXX	Al-Cu
3XXX	Al-Mn
4XXX	Al-Si
5XXX	Al-Mg
6XXX	Al-Mg-Si
7XXX	Al-Mg-Zn
8XXX	All Other Types

corrosion resistance.[1,7] The 7XXX series aluminum alloys (Al-Mg-Zn-Cu), which were developed for high strength aircraft purposes, have desirable age-hardening character-istics, but in saline environments also have higher corrosion rates, increased pitting tendency, and in time suffer severe deterioration.[4,7]

Crevice corrosion can be a serious problem for some aluminum alloys exposed to a sea water environment. Rosenfeld and Marshakov[8] found severe crevice corrosion in certain aluminum alloys when exposed to a saline solution. According to Goddard et al.[4] the 2XXX and 7XXX series aluminum alloys exhibit poor corrosion resistance in sea water.

This study explores the mechanism of crevice corrosion of Al-Mg-Zn and Al-Mg-Zn-Cu alloys in a 3.5% NaCl solution. Comparison is made of the behavior of a ternary Al-Mg-Zn alloy and two Al-Mg-Zn-Cu alloys on the basis of variations of electrode potential, current flow between the crevice and

the outside surface, and crevice solution chemistry changes as functions of time. The investigated phenomenon is that of corrosion in macroscopic crevices in which microstructural features affect the corrosion conditions by their presence, but where the cell size is large compared with the grain size.

CHAPTER II

REVIEW OF THE LITERATURE

Crevice Corrosion

Early literature dealing with crevice corrosion tends to focus on the mechanisms thought to be responsible for the corrosion processes. Many such theories of the mechanism of crevice corrosion have been forwarded over the last fifty years; however, only a few have survived: (1) the hydrogen cell,[9] (2) the metal-ion cell,[10] and (3) the differential aeration cell.[11]

It has been demonstrated that any of these cells can cause crevice corrosion in selected materials under special circumstances. Rosenfeld et al.[12] proposed that general crevice corrosion may involve more than a single mechanism, and possibly several separate mechanisms occuring simultaneously. Fontana and Greene[13] developed a crevice corrosion model that incorporated the prevalent corrosion mechanisms mentioned previously; it is shown in Figure 1. The Fontana and Greene model, because of its good adaptability to various conditions, is used as a starting point for many crevice corrosion studies.[9]

It is generally accepted that crevice corrosion has certain aspects in common with both stress corrosion cracking
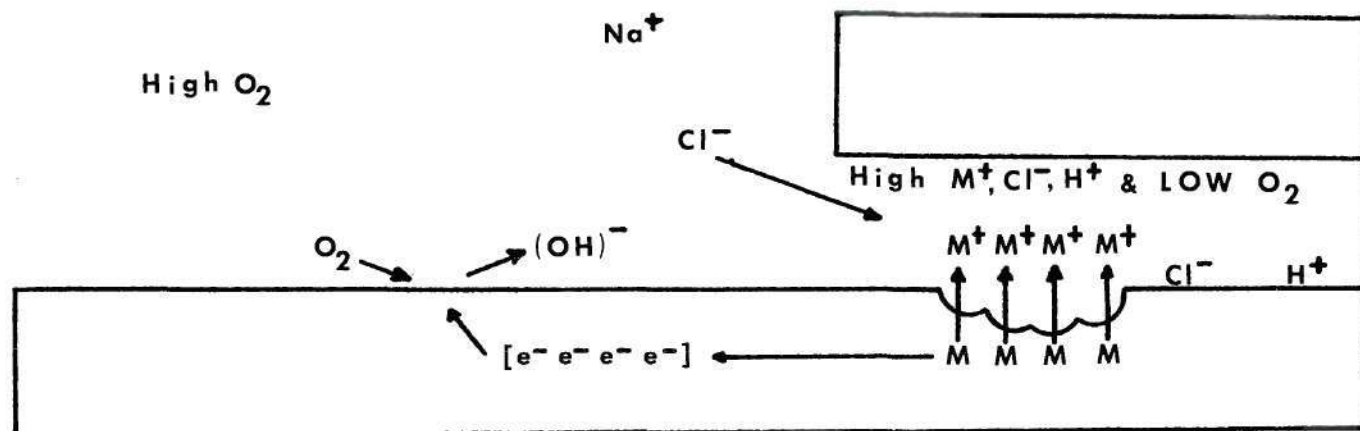
Figure 1. The Fontana and Greene Model of Crevice Corrosion.

(SCC) and pitting corrosion. Pitting is similar to crevice corrosion except for the cell size and method of sustaining the corrosion process.[14,15] Stress corrosion cracking has common features with crevice corrosion because a crack is also a crevice.

In aqueous environments which are open to the atmosphere, depletion of dissolved oxygen occurs in the crevice as the oxygen is consumed in cathodic reactions and its transport into the crevice is restricted. The primary anodic and cathodic reactions taking place on the electrodes of a crevice cell are then the following:

On the outside surface

$$O_2 + 2H_2O + 4e^- \rightarrow 4(OH)^-$$ 　　　　cathodic reduction of oxygen

On the crevice surface

$$M \rightarrow M^{n+} + ne^-$$ 　　　　anodic dissolution of the metal

$$M^{n+} + xH_2O \rightarrow M(OH)_x^{(n-x)+} + xH^+$$ 　hydrolysis of metal ions

$$2H^+ + 2e^- \rightarrow H_2$$ 　　　　hydrogen evolution (cathodic)
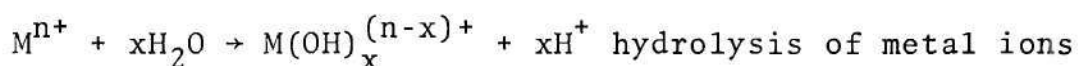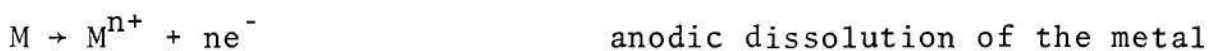
Crevice Corrosion in Aluminum Alloys

Goddard et al.[4] states that very little information is published on crevice corrosion of aluminum alloys because of the difficulty encountered in laboratory investigation. He also states that crevice corrosion of aluminum and its alloys is negligible in the atmosphere, although crevice corrosion of aluminum alloys can be severe in sea water.

France[9] observed that crevice corrosion in aluminum alloys was closely associated with the salt concentration in the environment. Rosenfeld and Marshakov[8] found that the corrosion rate inside a crevice on an aluminum alloy was about ten times greater than the corrosion rate on the outside surface.

The following sequence of events is thought to lead to crevice corrosion of aluminum alloys:[8,9,14,16,17]

1. Depletion of dissolved oxygen in the crevice results in formation of a differential aeration cell.

2. Metal ion concentration in the solution within the crevice increases.

3. Acidification of the crevice solution occurs as a result of hydrolysis; the pH of the solution decreases.

4. Chloride ions move into crevice to preserve electroneutrality.

5. Hydrogen reduction stabilizes the pH of the crevice solution; hydrogen gas evolves.

Crevice Solution Chemistry

Fujii[18] stressed the importance of the study of the solution chemistry in determining the mechanism (or mechanisms) involved in the corrosion process. The primary hindrance to analysis of the crevice solution is the inaccessibility and

the small volume of solution.[18] Proper cell design in laboratory experiments is therefore of great importance. The cell designs used in various studies of localized corrosion were reviewed by Fujii.[18] Several techniques have been used for sampling and analysis of the solution in small cells. The freezing method,[19] which retards the chemical processes until the solution can be removed and analyzed, has been utilized to some success in studies of SCC[20] and crevice corrosion. Other techniques have been developed, such as the employment of microcapillaries to obtain the crevice solution,[21] and the use of implanted electrodes and pH probes to monitor the chemical changes within the crevice.[18]

Analytical Methods

The analysis of the crevice solution for ionic composition is difficult because of the small amount of solution available. The primary technique used so far for detecting ions in solutions has been colorimetry. This technique can also be used to determine concentrations; however, the small amount of solution available from crevices limits the amount of information that can be obtained from a single sample of solution.

Recently, Atomic Absorption Spectrophotometry has been used to detect and determine the concentration of metallic ions. An AA spectrophotometer using flameless atomization

in a carbon rod furnace has the capability to analyze
diluted samples of solution of a volume of only 5ul or less,
and to determine accurately the concentration by comparison
to known standards.[22]

Specific ion electrodes of several types have been
developed for the measurement of the concentrations of
various cations and anions in solutions. The potential of a
specific ion electrode, as measured versus a reference
electrode, is a function of the concentration of the ions.
The technique is similar to the determination of pH by means
of a glass electrode.

CHAPTER III

EXPERIMENTAL METHODS

Sample Preparation

The aluminum alloys were received, courtesy of the Aluminum Company of America (ALCOA), in plates which had been cast, homogenized, scalped, and hot rolled at 398°C. The alloy compositions are given in Table 2.

Table 2. Composition of the Aluminum Alloys

Alloy Designation	Percent Composition				
	Cu	Mg	Zn	Al	Other
76	0.00	2.20	6.17	91.63	0.00
77	1.55	2.23	6.16	90.05	0.01
7050	2.55	2.21	6.31	89.65	0.28

The samples were cut from the plates, trimmed to size, solutionized at 480°C for one hour, quenched in ice brine, and heat treated for nine hours at 120°C in a silicone oil bath. The heat treatment resulted in nearly maximum hardness at a point below the G. P. solvus line, as shown in Figures 2 and 3.[23,24,25,26]

Optical metallographic examination of the longitudinal sections of the three alloys revealed that the grain size of

alloy 7050 was substantially smaller than those of alloy 76 and 77, alloy 76 having the largest grains. Sanders[26] suggested that copper in excess of 1.5 per cent acted as a grain refiner. The microstructures of all three alloys are shown in Figure 4a, and a comparison of the estimated grain sizes is shown in Table 3.

Table 3. Estimated Grain Size of the Alloys

Alloy	Grain Size
76	194×10^{-3} mm^2
77	150×10^{-3} mm^2
7050	2×10^{-3} mm^2

The design of the crevice cell is shown in Figure 4b. The samples were mounted in acrylic plastic holders with insulated wires to provide an electrical connection between specimens, and bonded with an epoxy sealer. The exposed surface area of each electrode was 2 cm^2. The surface was then prepared by wet grinding through #600 grit silicon carbide paper. Cover plates of acrylic plastic and PTFE were machined to exact size and holes were drilled in the cover plates for the microcapillary or pH electrode. A PTFE spacer, 0.25 mm thick, provided the crevice width. The spacer and cover plate were secured to the plastic holder by means of nylon screws, as shown in Figure 4b.

The solution used in the study was an aqueous, nearly neutral, 3.5% NaCl; it was not stirred, and was open to the atmosphere. The solution covered the external electrode to a depth of about 1.5 cm.

All three alloys, 76, 77, and 7050, were tested in four chemical and electrochemical experiments dealing with crevice corrosion. Since crevice corrosion is a time dependent process, all experiments were conducted as a function of time. The following variables were measured:

(1) Electrode potentials;

(2) Galvanic currents between the electrodes;

(3) The acidity inside the crevice;

(4) Concentrations of metallic and chloride ions in the crevice solution.

Electrochemical Measurements

The samples were electrically connected, as shown in Figure 5, and the galvanic current flow between the two electrodes was measured by means of a potentiostat (PAR Model 174) adjusted for zero potential difference between the electrodes. The corrosion potentials of the electrode couple and of an uncoupled outside electrode were measured with respect to a standard saturated calomel electrode by means of an electrometer (Keithley Model 600B).

Measurements of pH

The acidity of the solution in the crevice was

determined by measuring the pH both continuously and by periodic sampling. The continuous monitoring method is shown schematically in Figure 6; a miniature glass electrode was mounted in the PTFE cover plate, and the acidity was measured with a pH meter (Leeds and Northrup Model 7415) and recorded on a strip chart recorder (Honeywell Electronix Model 194). For sampling, a nylon fiber-plugged 5ul capillary was inserted in the PTFE cover plate instead of the pH electrode, as illustrated in Figure 5. At the selected time, the nylon fiber was pulled out and the solution-filled capillary was removed; the pH measurement was made by means of an inverted pH electrode. The cup-shaped inverted pH electrode held the 5ul of solution which was touched with a reference microelectrode. This method preserved the 5ul of solution for further analysis.

Analysis for Metallic and Chloride Ions

The concentration of metallic ions in the crevice solution was determined using an AA spectrophotometer (Varian Techtron Model 1200) with a flameless atomization in a carbon rod furnace. The crevice solution was sampled at selected times using the nylon fiber-plugged capillary mentioned previously. The solution was diluted and analyzed for concentrations of Cu, Zn, Mg and Al. Chloride ion analysis was performed using an ion-selective solid state electrode after a suitable dilution of the sample.

Polarization Measurements

Anodic and cathodic potentiostatic polarization measurements were made on alloys 76, 77, and 7050 in the bulk 3.5% NaCl solution. The solution was deaerated with nitrogen for anodic measurements, and aerated with air for cathodic measurements. Anodic polarization measurements were also made on all three alloys in a bulk solution with characteristics of the crevice solution after 100 hours of exposure. All potentiostatic measurements were made using a Wenking Potentiostat Model 68TS3, and a Hewlett-Packard X-Y Recorder. The potential scanning rate was 20 mv/min.
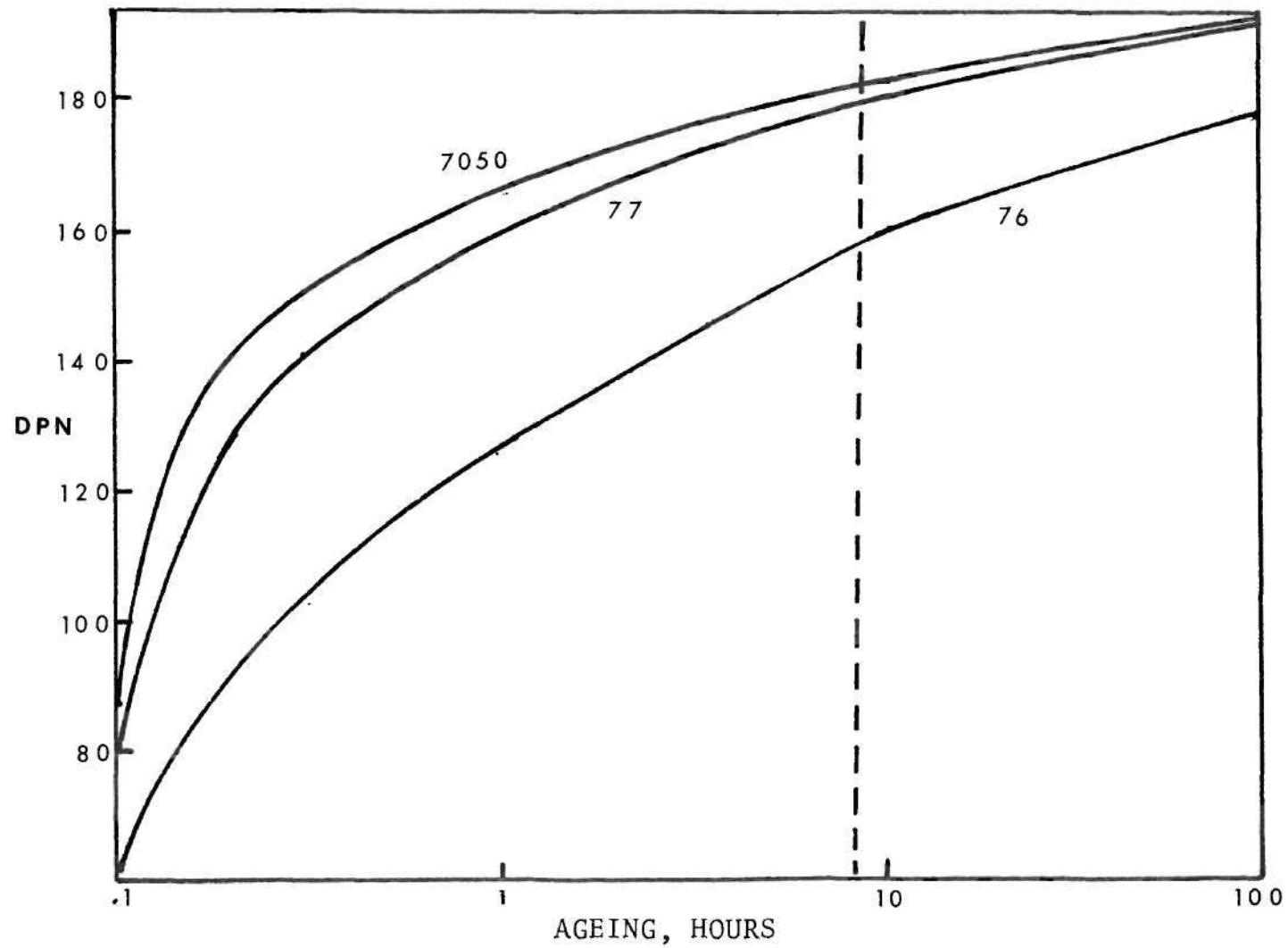
Figure 2. Hardness Curves vs. Ageing Time for Alloys 76, 77, and 7050. Ageing Temperature was 120 C. (25,26)
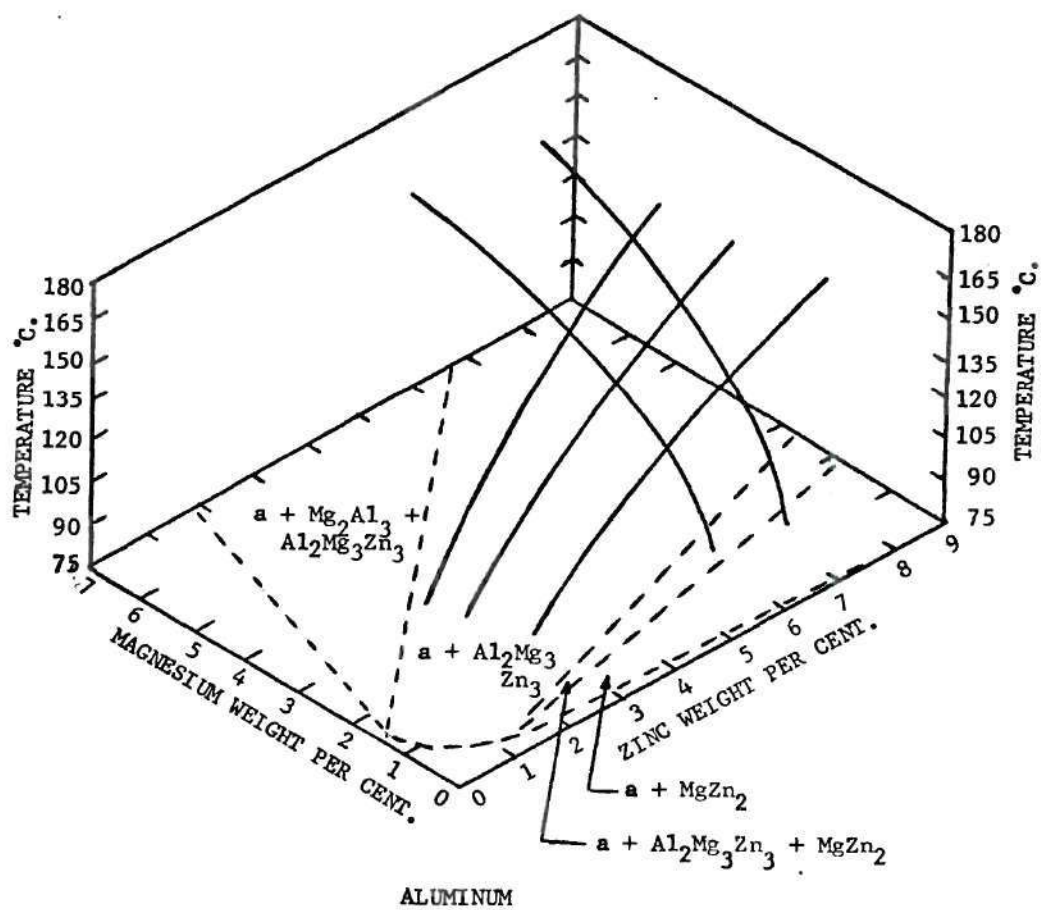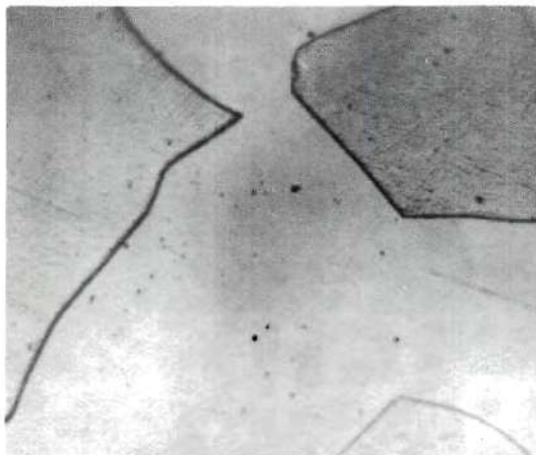
Figure 3. Upper Solvus Line for Al-Mg-Zn Alloys.[26]
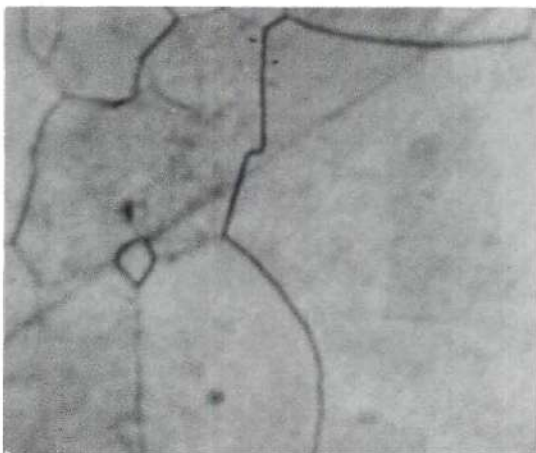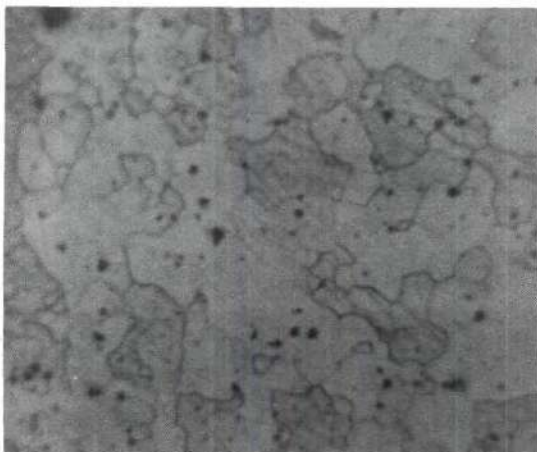
ALLOY 76

ALLOY 77

ALLOY 7050

Figure 4a. Microstructure of the Longitudinal Sections
of Alloys 76, 77, and 7050. (25,26)
Magnification: 100X.
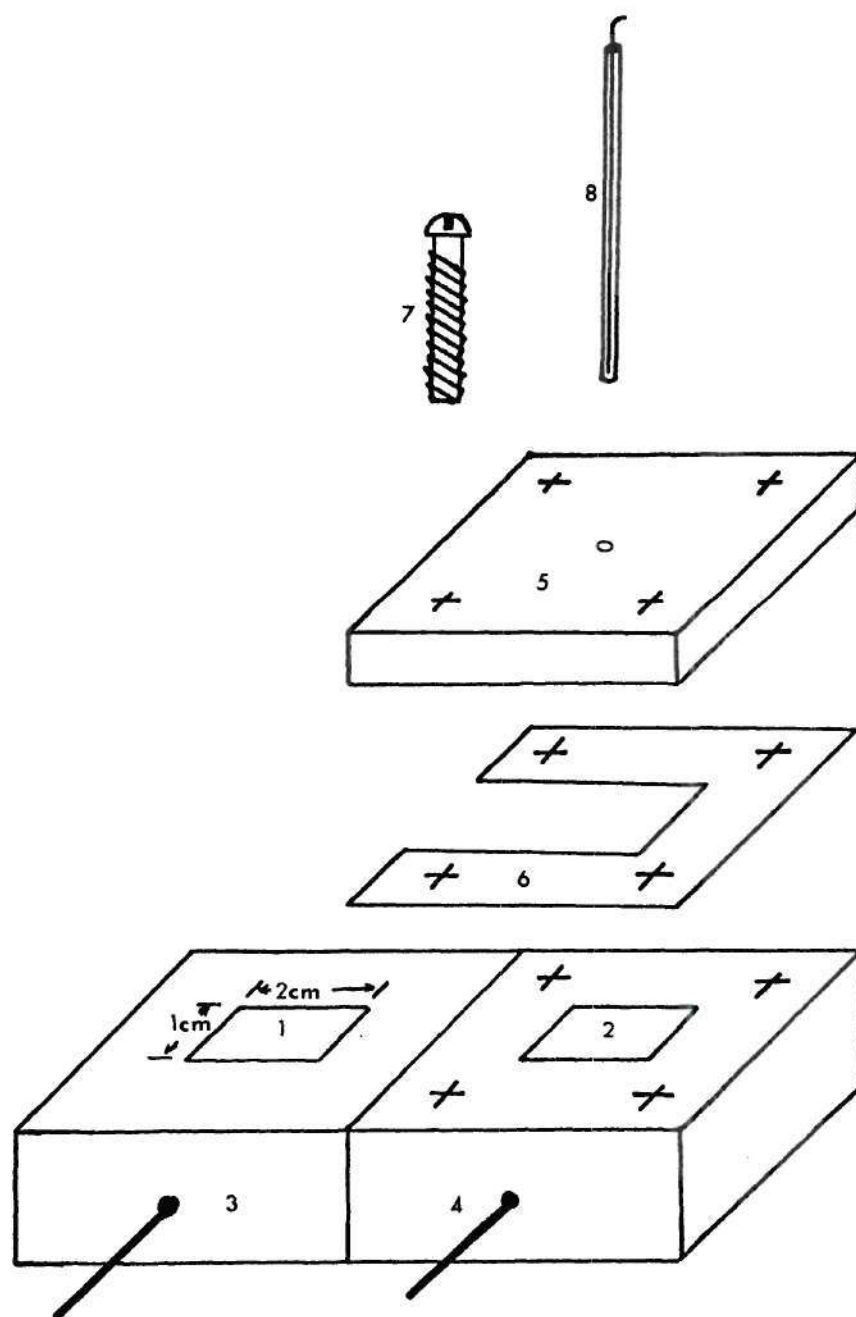
Figure 4b. Artificial Crevice Corrosion Cell. (1 and 2 - identical samples, 3 and 4 - electrical connections, 5 - PTFE or acrylic cover plate, 6 - PTFE spacer, 7 - one of four non-metallic screws, 8 - fiber plugged capillary.)
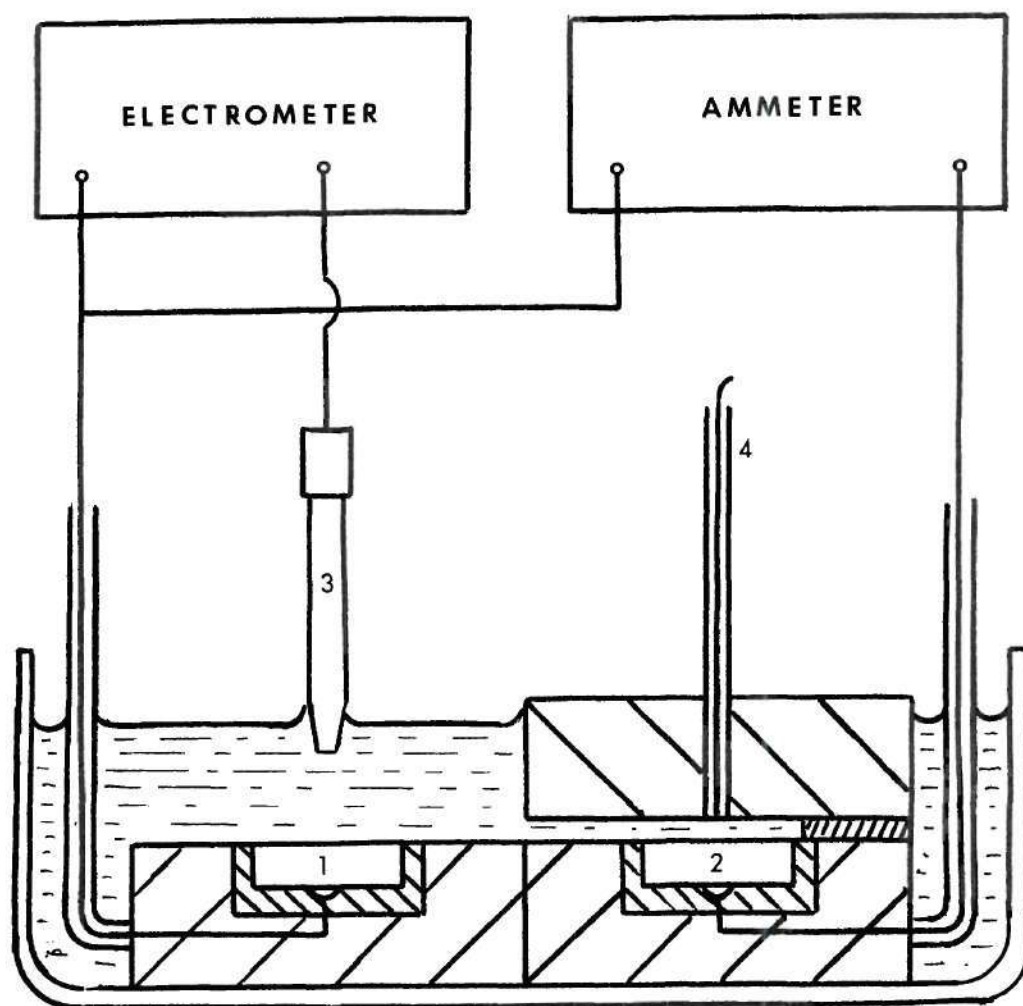
Figure 5. Schematic Set-up of a Corrosion Cell to
          Allow Sampling of the Crevice Solution
          and Measurement of the Current and Pot-
          ential. (1 and 2 - identical samples,
          3- reference electrode, 4 - capillary)

Figure 6.   Schematic Set-up of the Corrosion Cell to
Allow Continuous Monitoring of the pH of
the Crevice Solution.   (1 and 2 - identical
samples, 3 - reference electrode, 4 - pH
electrode)

CHAPTER IV

RESULTS

The crevice corrosion process on alloys 76, 77 and 7050
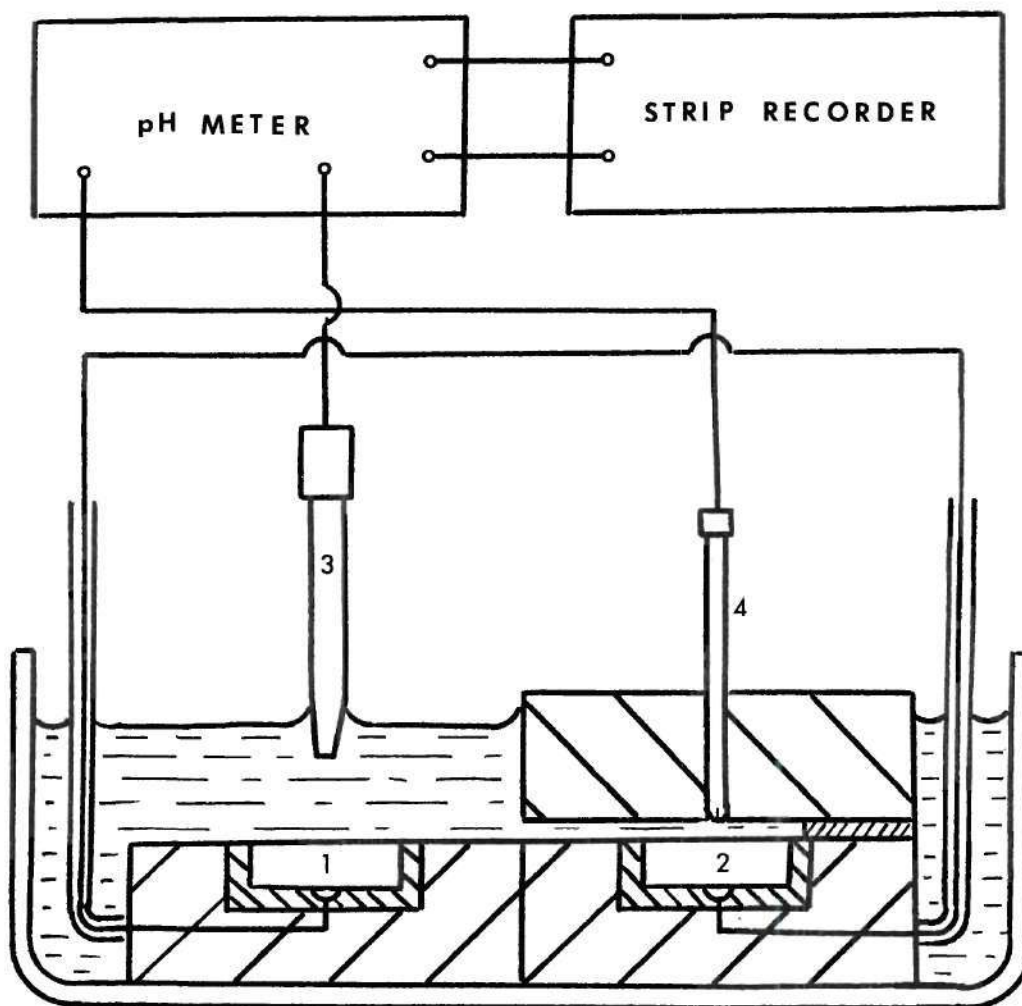was monitored for 100 hours. The most significant changes
occurred within the first 48 hours of exposure and the major
transitions occurred between hours six and thirty.

Visual Observations

The surface of all three alloys which were exposed to
the bulk solution showed visible corrosion damage, usually
in the form of pitting. The deterioration of alloys contain-
ing copper was substantially more severe than of the alloy
without copper. Surfaces of the copper-containing alloys
also showed moderate to heavy accumulation of dark corrosion
products, while the ternary alloy remained bright. The
conditions of the surface did not seem to be substantially
affected by the coupling with the electrodes placed inside
the crevice.

For all three alloys visual corrosion products were
less evident on the surface of the crevice than on the
outside electrode; however, pitting and grain boundary attack
were observed microscopically on all three alloys. The
severity of pitting increased with increasing copper content.
Micrographs of the various surfaces of all three alloys,

after an exposure of 100 hours, are shown in Figures 7, 8, and 9.

The formation of gas bubbles inside the crevice occurred early in each experiment, differing for each alloy only in initial starting time and quantity of gas, as shown in Figure 10. In eace case the gas gradually displaced the solution from the crevice. The rate of gas evolution was higher on alloy 76 than on alloys 77 and 7050. The results of the visual observations, together with main electro-chemical parameters, are summarized in Table 4.

pH Measurements

Figures 11, 12, 13 show the pH change in the crevice solution for alloys 76, 77, and 7050, respectively. In each case there was a slight initial increase in pH during early exposure, usually occurring within the first hour. Nearing the sixth hour of exposure a transition period began, resulting in a sharp drop in pH of the crevice solution. The pH decreased to about 3.8 regardless of the alloy, and an almost stable value was reached after about 30 hours of exposure. The bulk solution remained neutral throughout the experiments.

Electrochemical Measurements

The results of galvanic current measurement as a function of time are shown in Figures 11, 12, and 13. Initially, a current of about 2µA developed during the first

Table 4. Summary of Observations and Electrochemical Data

	ALLOY 76			ALLOY 77			ALLOY 7050		
	OUTSIDE	INSIDE	FREE	OUTSIDE	INSIDE	FREE	OUTSIDE	INSIDE	FREE
CORROSION PRODUCTS	Light	Very Light	Light	Mod.	Light	Mod.	Heavy	Light	Heavy
HYDROGEN GASSING	No	Yes	No	No	Yes	No	No	Yes	No
CURRENT FLOW (GALVANIC)	9.6 uA		None	10.2 uA		None	10.2 uA		None
POTENTIAL DIFFERENCE*	0.20 V			0.12 V			0.05 V		
MICROGRAPHIC CORROSION PRODUCTS	Light	None	None	Mod.	Mod.	Heavy	Heavy	Heavy	Heavy
PITTING	Mod.	Light	Light	Heavy	Mod.	Mod.	Heavy	Heavy	Heavy
GRAIN BOUNDARY ATTACK	No	Yes	No	No	Yes	No	No	Yes	No

* Maximum potential difference between the crevice and the freely corroding electrode.

hour of exposure, the surface within the crevice becoming the anode of the cell. The current remained constant during the initial period; when the pH transition began, the current increased and reached a stable value when the pH stabilized. For long periods of exposure, when the hydrogen gas displaces substantially the solution from the crevice, the galvanic current started to decrease. The maximum current following the transitions was higher for alloys with higher copper content; the differences, however, were small.

Electrode potential data are shown in Figure 14 as plots of potential versus time for crevice couples (mixed potentials) and freely corroding samples. In each case, the mixed corrosion potential of the crevice couple was more negative than the potential of the freely corroding single electrode. The highest difference between the potentials (crevice couple versus single electrode) developed at the end of the transition period. With increasing copper content the potentials were more noble, and the differences between the crevice couple and the single electrode decreased. The main parameters are summarized in Table 4.

Solution Chemistry

The results of the crevice solution analysis for ions of aluminum, zinc, copper, and magnesium, as a function of exposure time, are shown in Figures 15, 16, and 17, for alloys 76, 77, and 7050, respectively. At low exposure times the

concentrations of metallic ions were low. During the six to thirty hour transition period the concentrations of aluminum, zinc, and magnesium increased significantly and reached stable levels. The copper ion concentration remained very low. The concentrations of individual elements and their proportions in the solutions and the alloys are shown in Figures 15, 16, and 17.

The crevice solution of alloy 76 was analyzed for chloride ions. Figure 18 shows the Cl^- concentration as a function of exposure time. It increased during the test to about three times the initial value.

Polarization Measurements

The results of the polarization measurements are shown in Figures 19, 20, and 21 for alloys 76, 77, and 7050, respectively. Each graph shows the anodic and cathodic polarization curves in nearly neutral 3.5% NaCl (aerated for cathodic polarization and deaerated for anodic polarization), and anodic polarization curves in solution simulating the crevice solution after 100 hours of exposure. In the neutral solution the ternary alloy showed active anodic behavior, while the polarization curves of the copper containing alloys exhibited active-passive transitions; the alloy 7050 with highest copper content showed a more extensive passive region than the alloy 77. The cathodic current densities were substantially lower on the ternary alloy than on the alloys
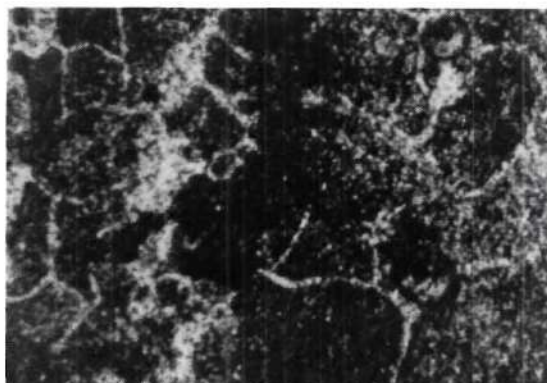
with copper. In the electrolyte simulating the crevice conditions none of the alloys exhibited passivity.
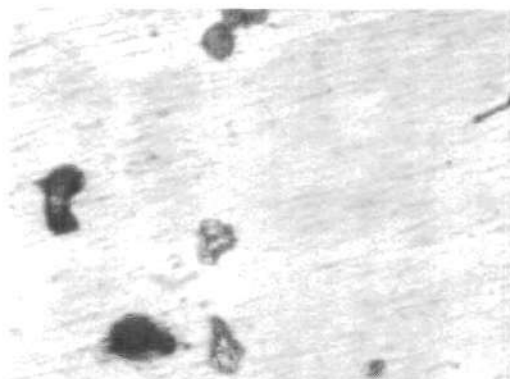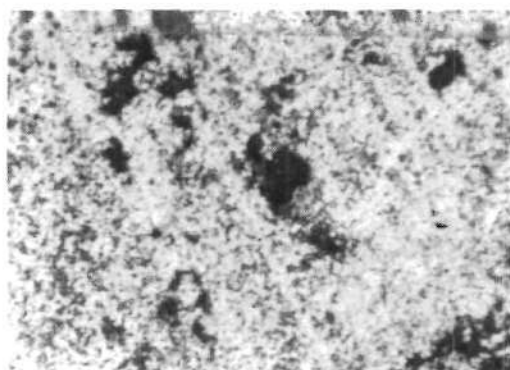
ALLOY 76
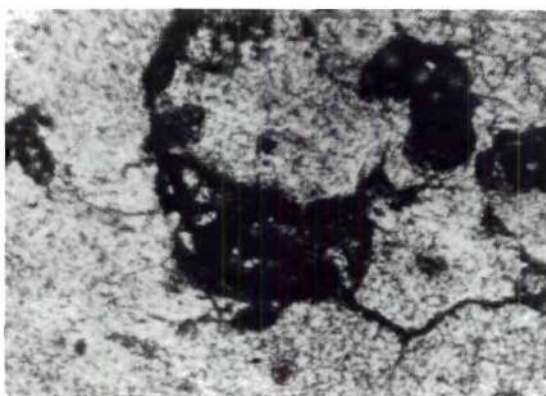
ALLOY 77

ALLOY 7050

Figure 7. Micrographs of the Electrodes in Crevices
after 100 Hours of Exposure (coupled).
Magnification: 100X.

ALLOY 76

ALLOY 77

ALLOY 7050

Figure 8. Micrographs of the Electrodes in the Bulk
Solution, coupled with Electrodes in a
Crevice, after 100 Hours of exposure.
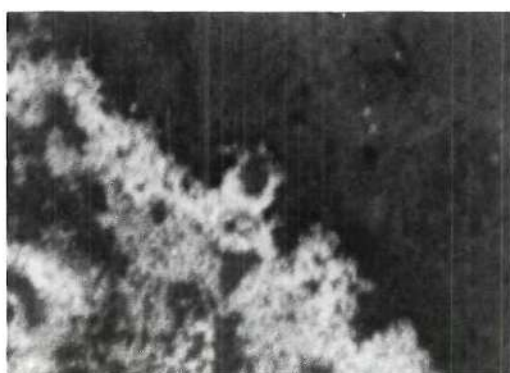Magnification: 100X.
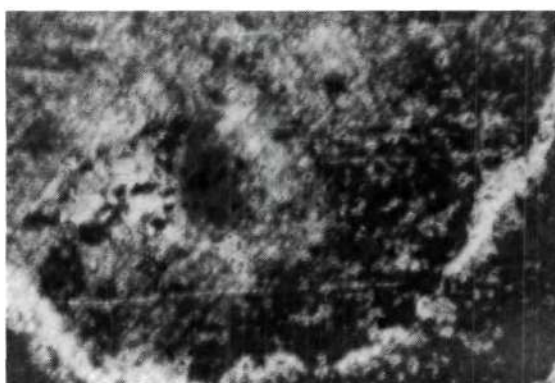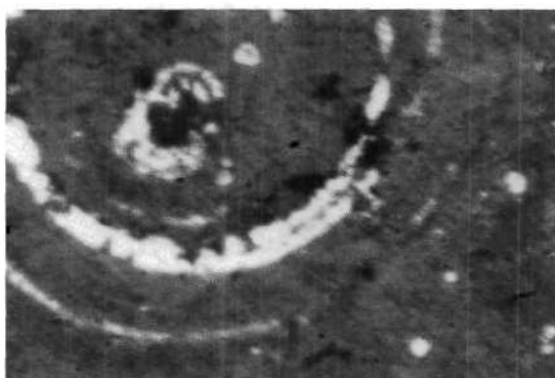
ALLOY 76

ALLOY 77

ALLOY 7050

Figure 9. Micrographs of the Freely Corroding
Electrodes, after 100 Hours of ex-
posure. Magnification: 100X.
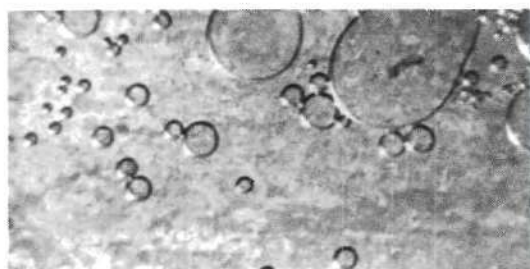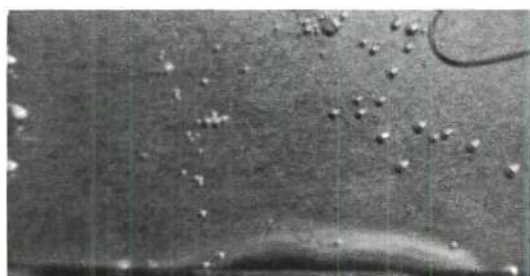
ALLOY 76

ALLOY 77

ALLOY 7050

Figure 10. Corroding Crevice Electrodes after
Twelve Hours of Exposure.
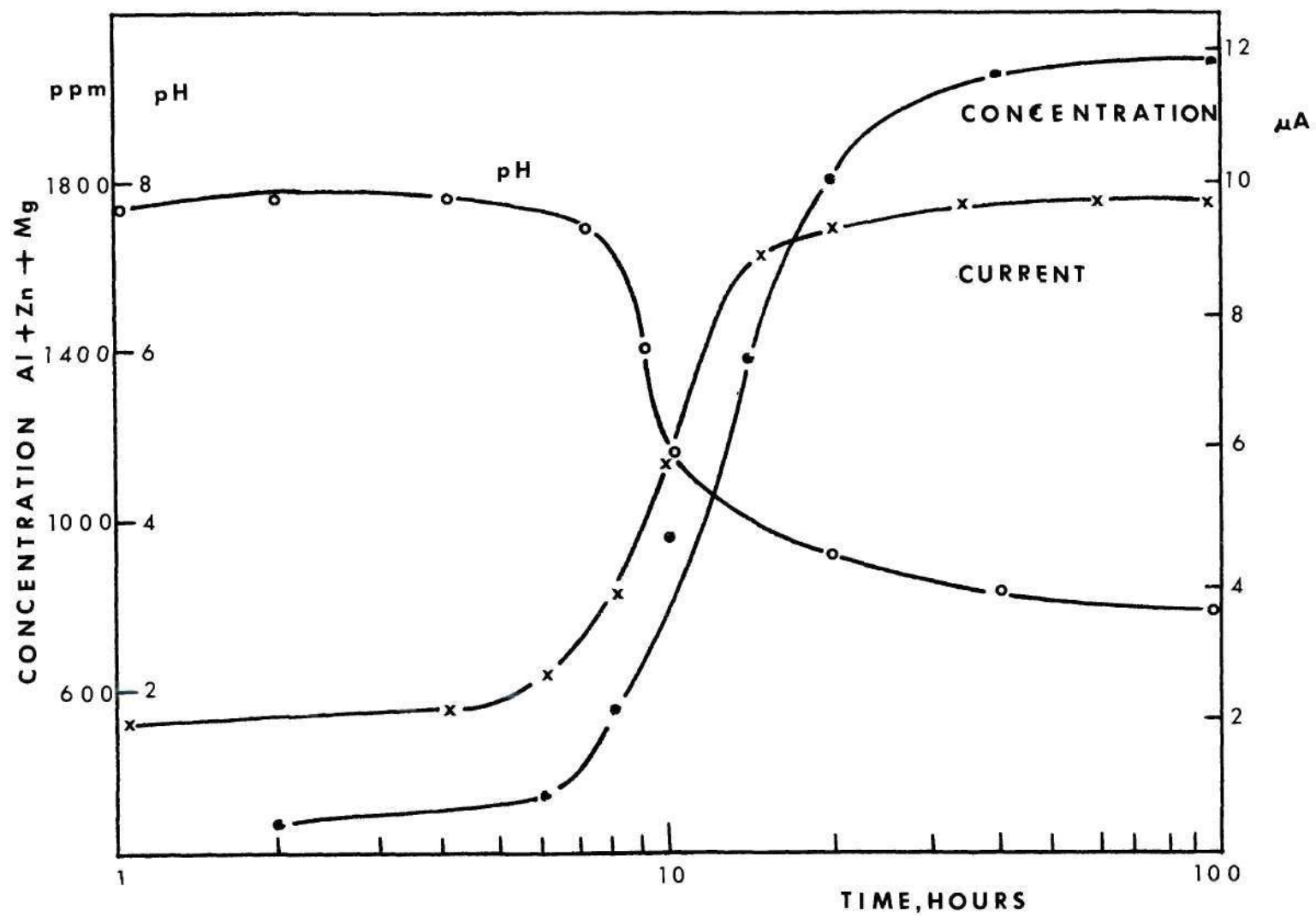
Figure 11.   Results of Current and Solution Chemistry Measurements
on a Crevice in Alloy 76.
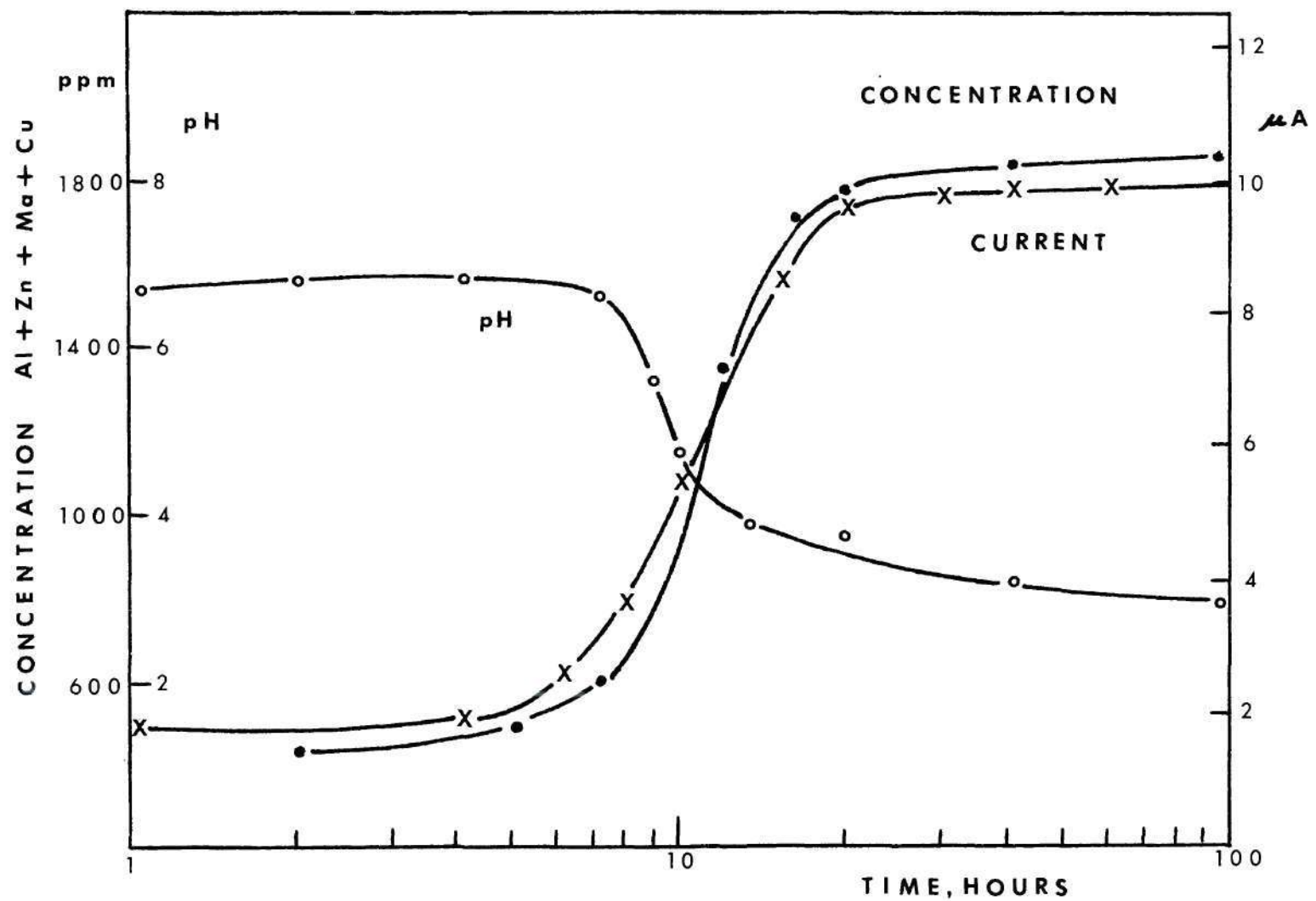
Figure 12. Results of Current and Solution Chemistry Measurements on a Crevice in Alloy 77.
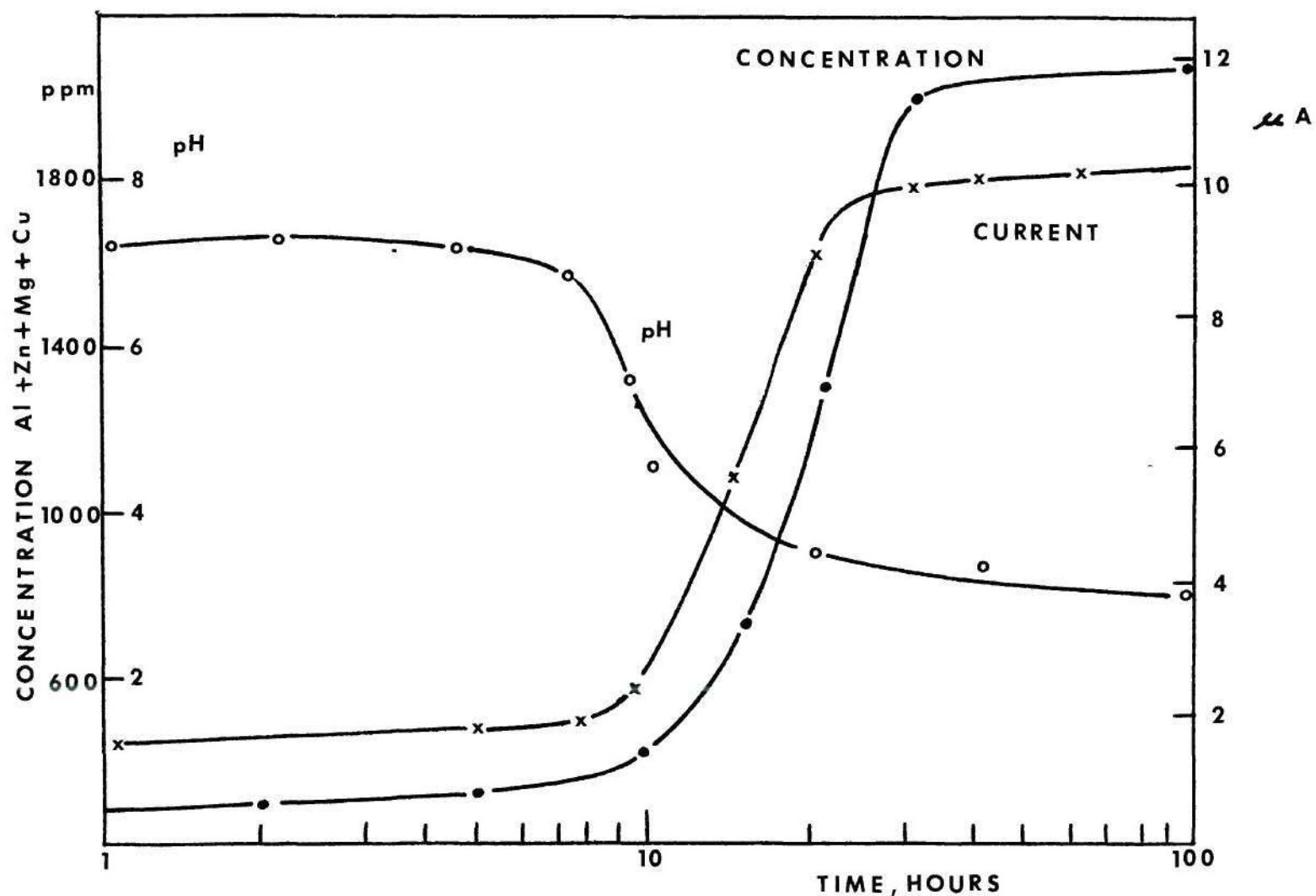
Figure 13. Results of Current and Solution Chemistry Measurements
on a crevice in Alloy 7050.
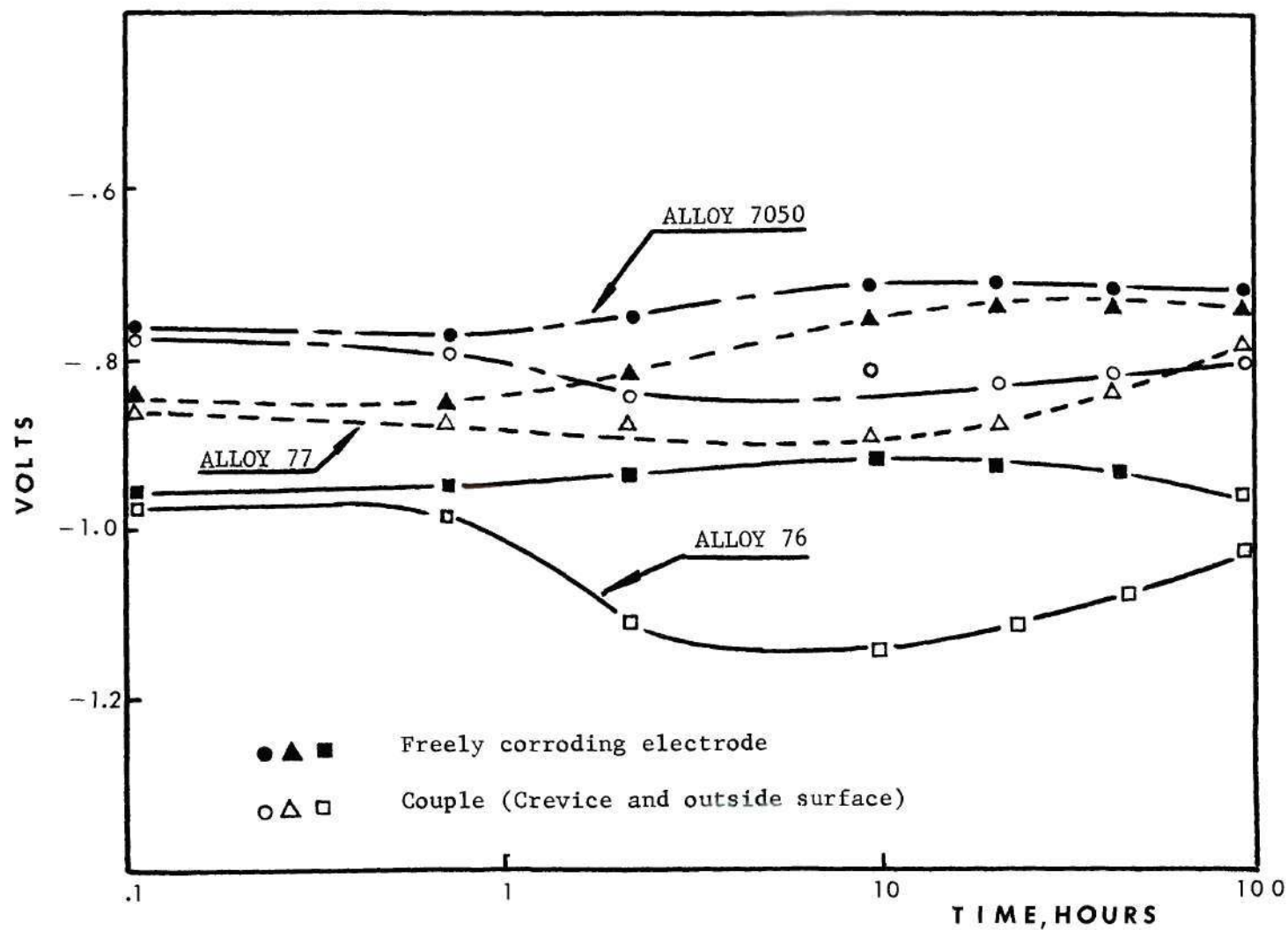
Figure 14. Corrosion Potential of Freely Corroding Samples of
Alloys 76, 77, and 7050, and of Crevice Couples, in
Aerated 3.5% NaCl.

34
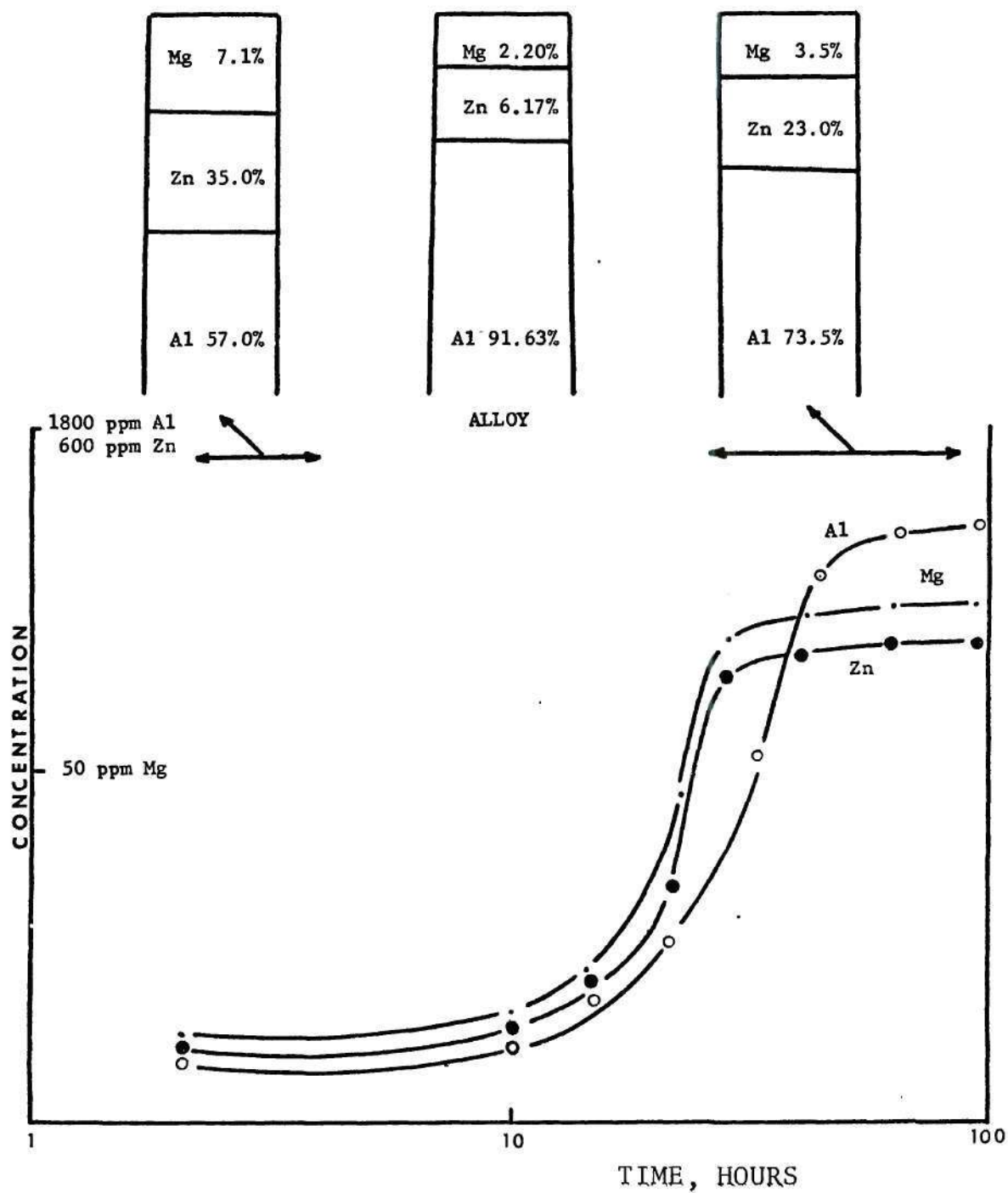
Figure 15. Concentration of Aluminum and Alloying Elements in the Crevice Solution of Alloy 76 as a Function of Time.

Cu .02%
Mg 4.8%
Zn 9.0%
Al 86.2%

Cu 1.6%
Mg 2.2%
Zn 6.2%
Al 90.0%

Cu .02%
Mg 3.9%
Zn 15.7%
Al 80.4%

ALLOY

1800 ppm Al
600 ppm Zn

CONCENTRATION

Al

Mg

Zn

50 ppm Mg
1.0 ppm Cu

Cu

1   10   TIME, HOURS   100

Figure 16.   Concentration of Aluminum and Alloying Ele-
ments in the Crevice Solution of Alloy 77
as a Function of Time.
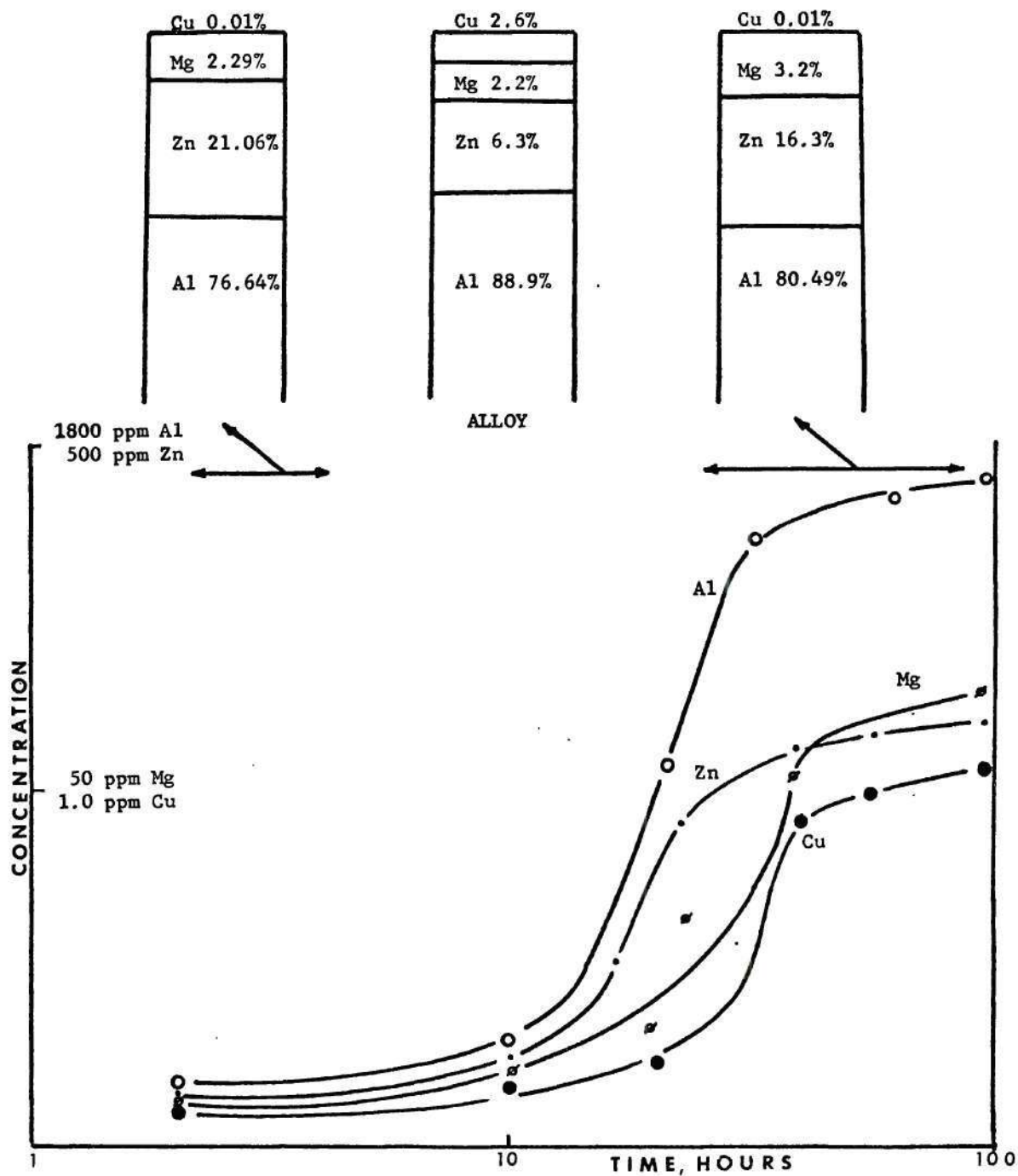
Figure 17. Concentration of Aluminum and Alloying Elements in the Crevice Solution of Alloy 7050 as a Function of Time.
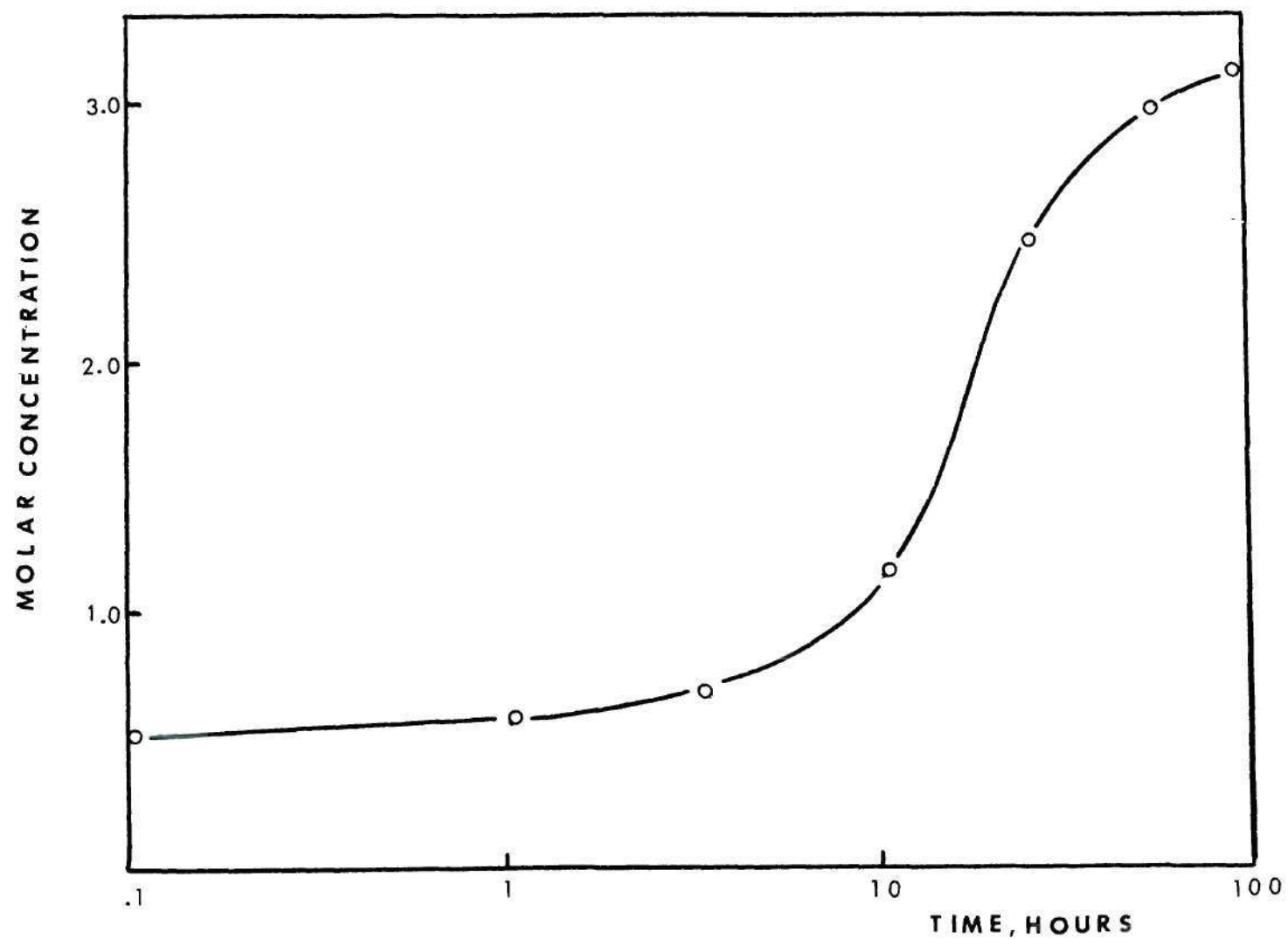
Figure 18. Chloride Ion Concentration in the Crevice
Solution on Alloy 76.
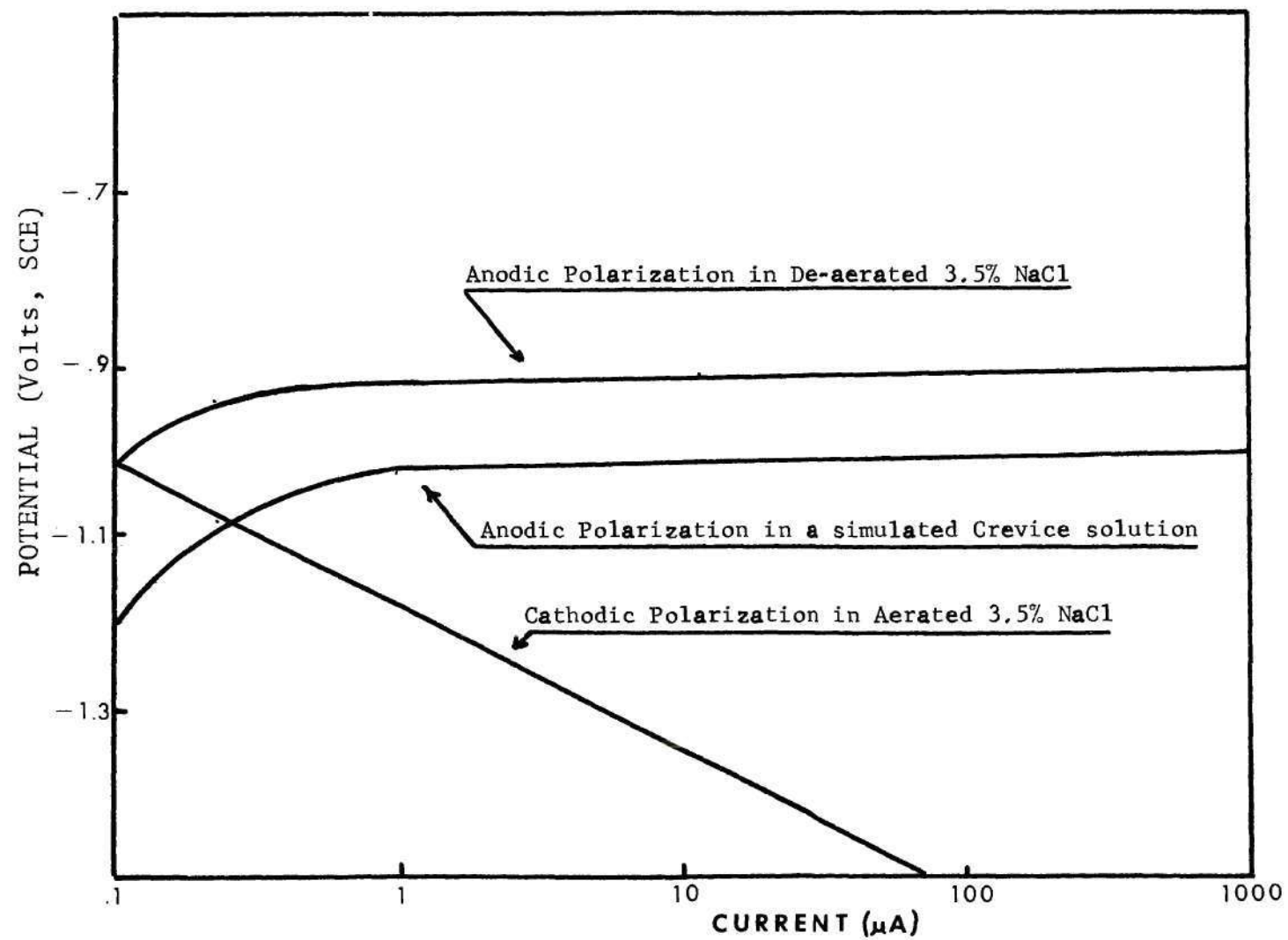
Figure 19.   Polarization Curves of Alloy 76.
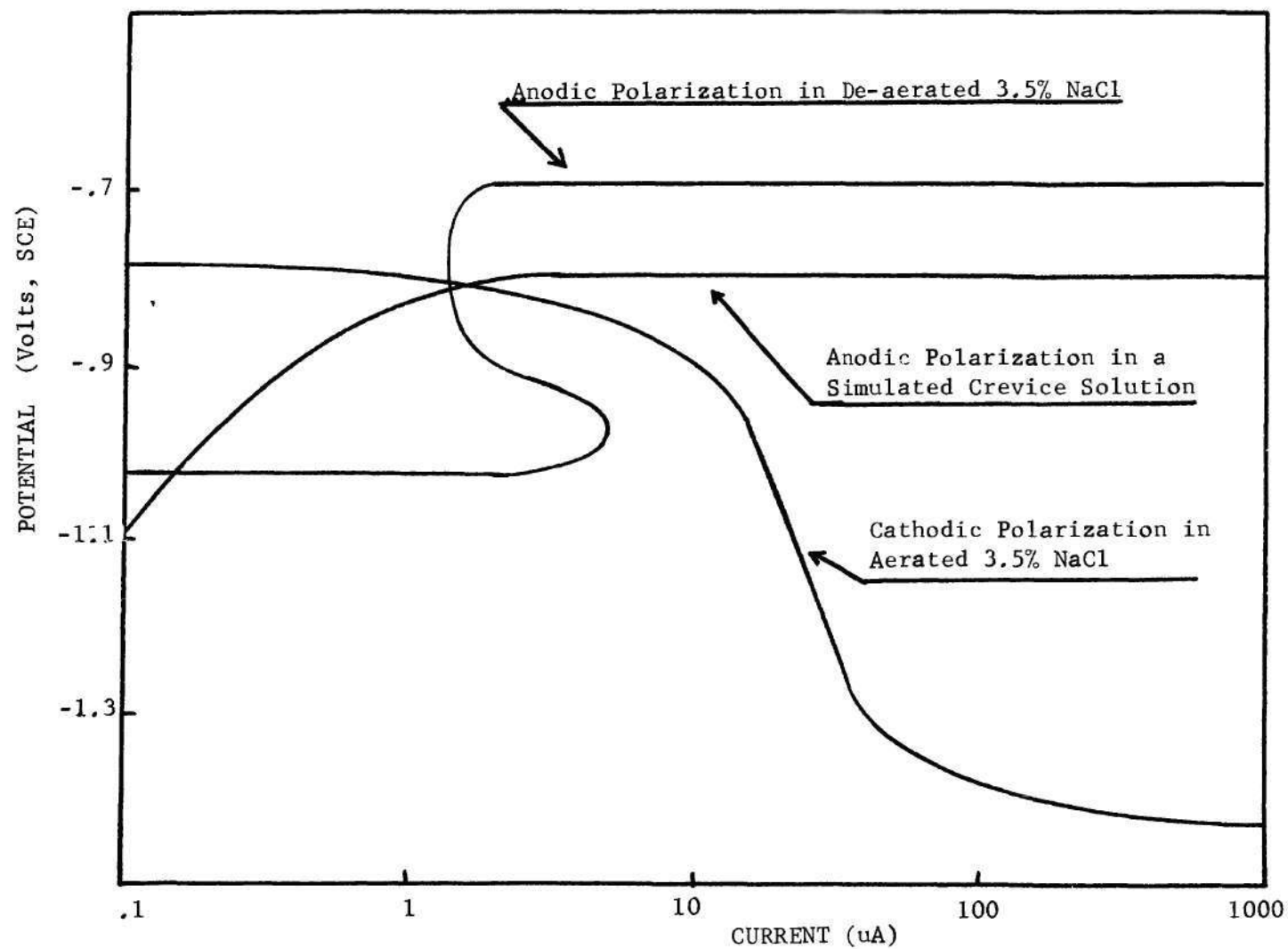
Figure 20. Polarization Curves of Alloy 77.
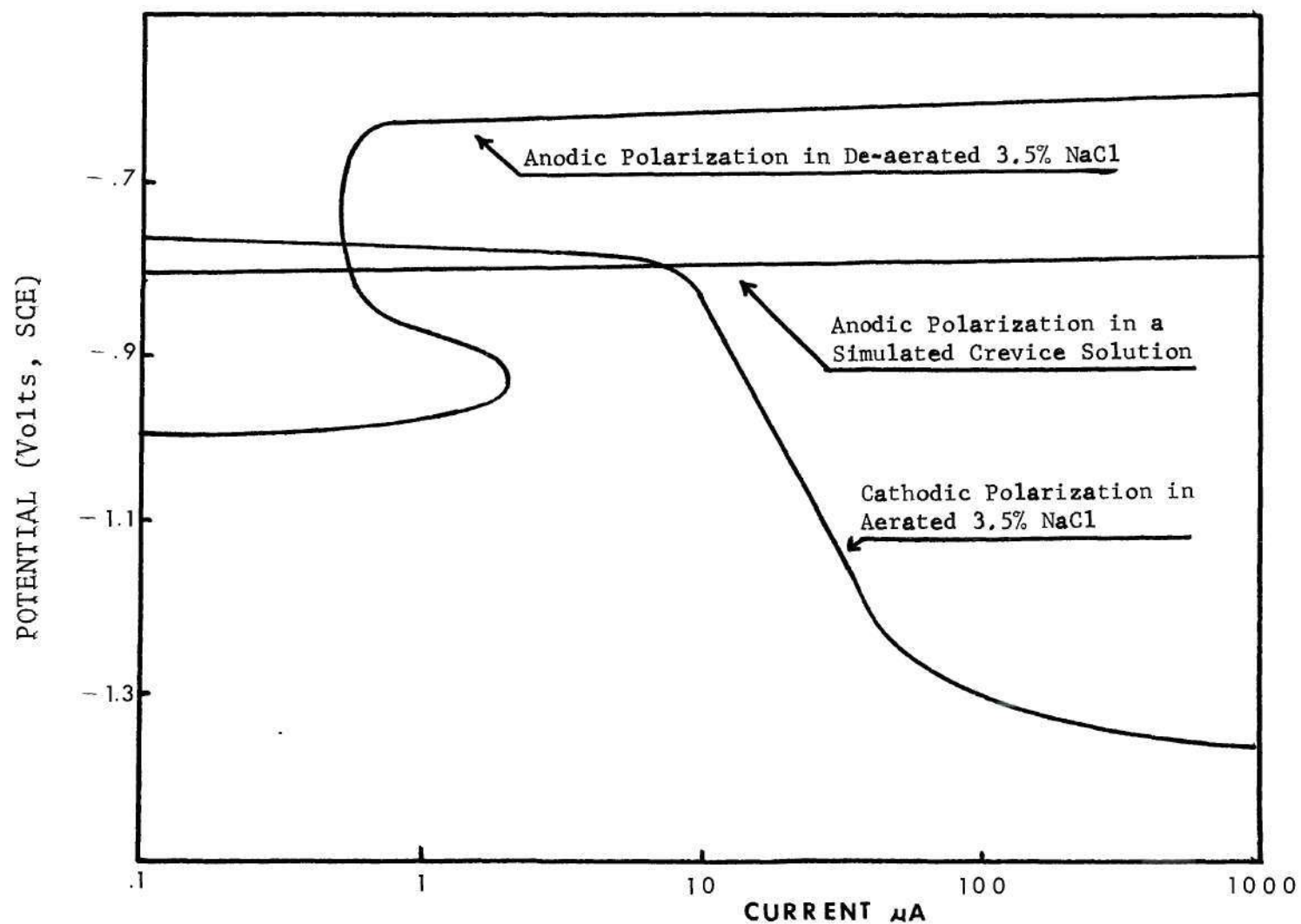
Figure 21. Polarization Curves of Alloy 7050.

CHAPTER V

DISCUSSION OF RESULTS

Crevice Corrosion in Al-Zn-Mg-Cu Alloys

The results of the corrosion tests on freely corroding samples showed the well known effect of copper on the corrosion resistance of aluminum alloys in chloride environments;[7] the copper containing alloys suffered heavy attack, both general and localized, while the ternary alloy corroded significantly less. The difference can be explained by the effect of copper on the cathodic reactions; cathodic polarization curves (Figures 19, 20, and 21) show that cathodic current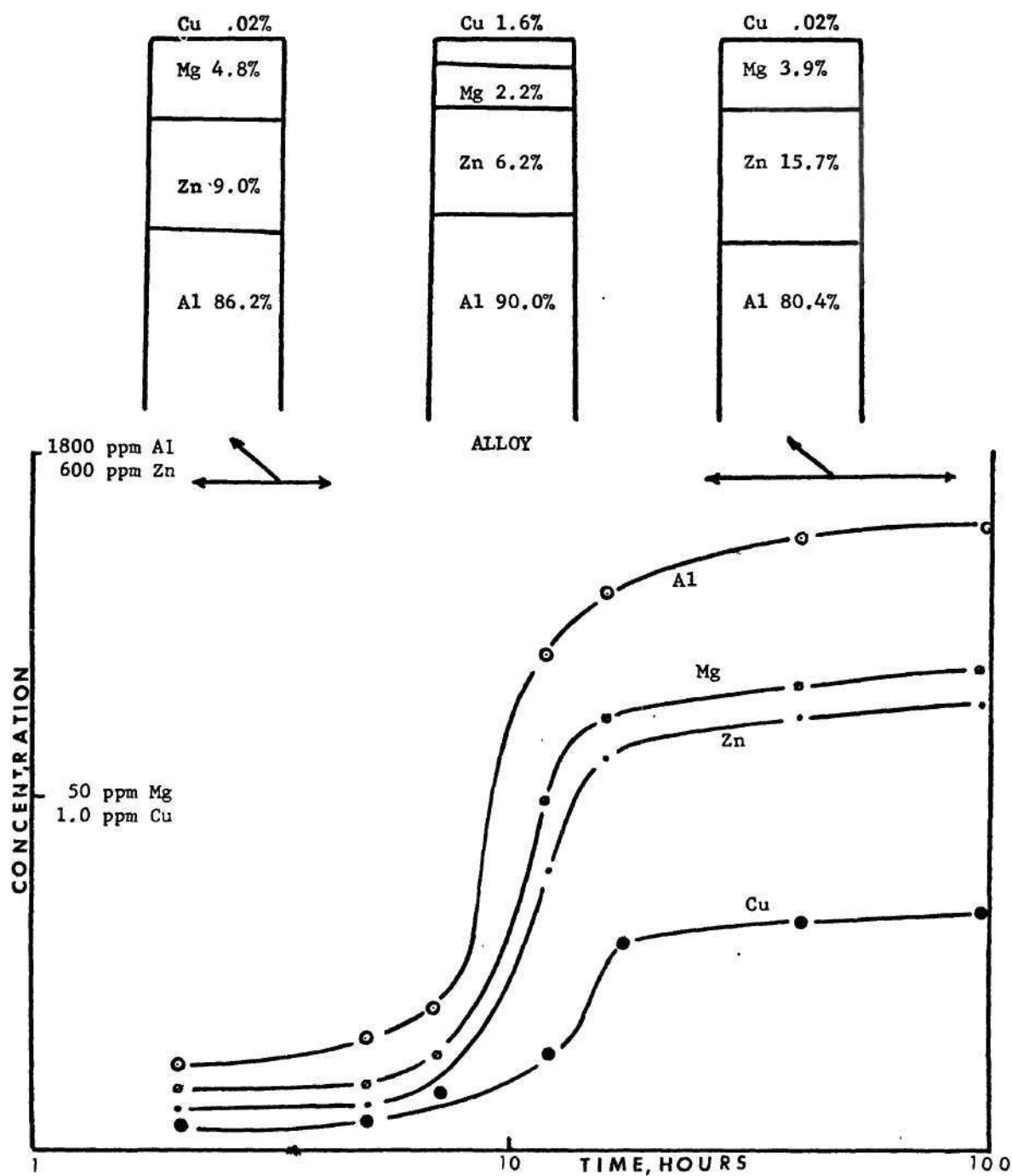s are substantially higher on alloys with copper. Although the anodic polarization curves in neutral 3.5% NaCl show that the addition of copper results in the appearance of a passive region, and that the pitting potential increases with copper content, the heavy pitting observed on freely corroding samples shows that actual pitting potentials were lower than the potentiodynamic polarization curves indicate. On the ternary alloy the low rate of the cathodic reaction controlled the corrosion rate.

The results on crevice couples were in general agreement with modern theories of crevice corrosion.[9,14,15] A macro-cell, with the anode inside the crevice, formed early

in each test, evidently due to the depletion of oxygen in the crevice by cathodic reduction. This also caused a slight increase in the pH of the crevice solution. In the initial period the potential differences were small, and the cell current was very low. Higher potential differences and currents developed during a transition period, which started after about six hours of exposure. The kinetics are, however, a function of the geometry of the crevice and the time scale is thus valid only for the geometry used in the tests.

The results of the solution chemistry analysis showed that the main factor in the transition was the acidification of the solution within the crevice. The acidity changed from the initial, almost neutral, value, to a new steady state value of pH 3.8, regardless of the type alloy, and in good agreement with published data.[8]

The potential of the crevice couple changed during the transition to a more negative value, as compared with the freely corroding electrodes. The largest difference was observed on the ternary alloy, and the smallest on the alloy with highest copper content (see Table 4). At the same time, the current between the electrode in the crevice and in the bulk solution increased to about 50 $\mu A/cm^2$; the current density was higher for higher copper content, but the differences were small. The increase in the current with copper content, despite the decrease of the potential difference, can again

be attributed to the higher cathodic current densities on alloys with copper.

Within the crevices on copper containing alloys the accumulation of corrosion products and pitting were less severe than on the external electrodes; on the other hand, grain boundary attack was substantially increased within the crevices. Grain boundary attack was also observed in the crevice on the ternary alloy; pitting, however, was relatively light. The corrosion deterioration of the external electrodes was less severe than that of the freely corroding samples, but still substantial on alloys with copper. The reduction in the rate of attack can be attributed to the lowering of the electrode potential; the effect was not sufficient to prevent pitting, but the rate was decreased.

The main factor of the corrosion condition within the crevices was the sharp increase in acidity. Chloride ion concentration also increased, but the build-up was slower and less severe. The effect of the solution chemistry on the corrosion behavior can be evaluated by comparing the anodic polarization curves in neutral 3.5% NaCl and in acidified solution (pH 3.8) with increased chloride content (Figures 19, 20, and 21). In each case, the change resulted in an increase in anodic currents. For alloys containing copper, the change also caused elimination of the passive region. This is in agreement with the Pourbaix diagram for system aluminum-water, which shows that in solution more acidic than

pH 4 the passive film becomes unstable and the metal corrodes actively.[27]

The crevice corrosion effects examined in this work were basically macroscopic, the cell size being large compared to the dimensions of the microstructure, such as grain size. In a macrocell the microstructure affects the corrosion conditions by the presence of the phases, but their distribution does not play a significant role. This assumption is valid only as long as there is no significant localized attack on the electrode surfaces; when pitting and/or grain boundary attack occur, local microcells form and the corrosion conditions become non-uniform. Localized corrosion was observed on the electrodes in this study, but the exposure times were relatively short and microcells were only initiated.

Aluminum alloys are very susceptible to non-uniform corrosion which can have the form of pitting, selective dissolution of phases, grain boundary attack, stress corrosion cracking, etc. These forms of corrosion are associated with formation of microcells in which the conditions depend on the composition and distribution of phases, such as precipitates, grain boundary zones, etc. A study of these effects was out of the scope of this work, but deserves detailed examination.

The Mechanism of Crevice Corrosion

On the basis of the experimental observations and the model proposed by Fontana and Greene,[13] the following

sequence of events is suggested for the crevice corrosion process in alloys studied in this work (Figure 22).

1. After initial immersion in 3.5% NaCl, micro-cells are set up on surfaces both outside and within the crevice. Galvanic current is near zero, corrosion potential is the same as the free corrosion potential, the metal ion concentration and pH are that of the bulk solution.

2. General corrosion takes place; products of corrosion are $(OH)^-$ for oxygen reduction (cathodic reaction) and metallic ions (Al^{3+}) (anodic reaction). The formation of $(OH)^-$ results in a pH increase in the crevice. The change of pH stops when the oxygen in the crevice solution is depleted.

3. Due to restriction of transport in a narrow crevice, Al^{3+} ions accumulate. When the solubility of $Al(OH)_3$ is reached, precipitation starts and the pH begins to drop as a result of the reaction;

$$Al^{34} + 3H_2O + 3e^- = Al(OH)_3 + 3H^+$$
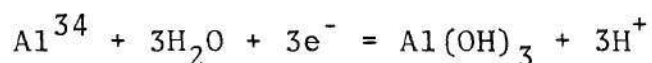
4. Chloride ions move into the crevice.

5. High acidity and high chloride content of the solution result in the destruction of the protective film. Highly anodic regions, grain boundaries and $MgZn_2$ precipitates are attacked preferentially. On the external surfaces corrosion continues at a slightly reduced rate.
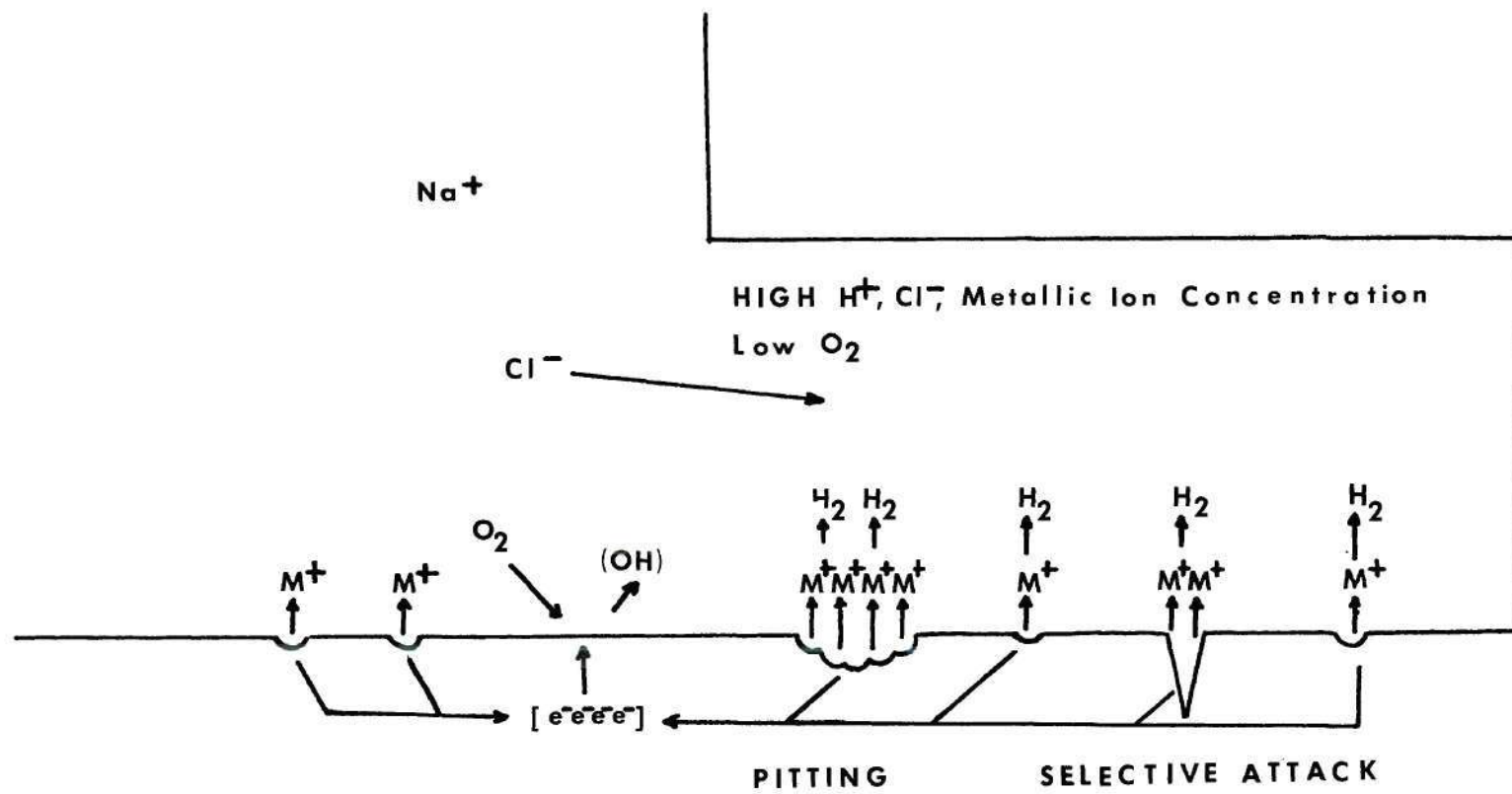
Figure 22. Crevice Corrosion Model for Al-Mg-Zn Type
Alloys Based on the Fontana and Greene Model.

47

6. As the acidity increases, hydrogen reduction begins to take place ($H^+ + e^- \rightarrow 1/2H_2$). Higher acidity probably develops in pits and in other sites of localized attack (e.g. at the grain boundaries) resulting in hydrogen evolution from specific points.

7. Hydrogen reduction and interdiffusion stabilizes the pH, and hydrogen gas begins to displace the crevice solution. The galvanic current peaks and starts to decrease as the effective surface area is reduced by gas. The crevice corrosion process slows down; localized corrosion continues on the outside surface.

Crevice Solution Chemistry

The increase in acidity of the solution within a crevice has been explained by hydrolysis of the metal ions.[10] The acidification starts when the solubility product of the least soluble salt is reached. For aluminum in neutral or alkaline solutions, as was the case in the initial period of the tests in this work, the following reaction is applicable:[28]

$$Al_2O_3 + H_2O = 2Al(O_2)^- + 2H^+ \qquad (1)$$
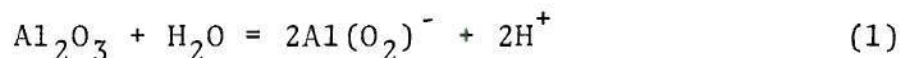
for which, according to Pourbaix,[27]

$$\log (AlO_2^-)(H^+) = -10.64 \qquad (2)$$

assuming the amorphous aluminum hydroxide as the precipitated form; then

$$\log (AlO_2^-) = -10.64 + pH \tag{3}$$

In the initial period, the concentration of aluminum ions in the crevice solution should not exceed the value given by equation (3).

The analytical data for a one hour exposure have given values 3.1, 38.9, and 11.9 times higher than the calculated values for alloys 76, 77, and 7050, respectively, as shown in the Appendix. The discrepancy can be a result of several factors or their combinations:

1. An error in pH determination. According to the calculations (see Appendix) the pH values which would be in agreement with the measured concentrations of aluminum after the one hour exposure would have to be as follows:

Alloy 76: pH 8.1 instead of the measured pH 7.6;

Alloy 77: pH 9.3 instead of the measured pH 6.7;

Alloy 7050: pH 8.2 instead of the measured pH 7.1.

In view of the experimental difficulties involved in measuring the pH of very small amounts of the crevice solution, certain error in pH values was possible. The difference shown above are, however, higher than expected for experimental error.

2. Inaccuracy of the published data for the solubility

product. There is substantial variation in the data in the literature.

3. An increase in the solubility due to the presence of chloride ions. The values of solubility given by Pourbaix[27] are for the system aluminum-water. According to Pourbaix, cations $Al(OH)^{++}$ and $Al(OH)_2^{+}$ may be present in the presence of chlorides; they may account for the higher amounts of aluminum found in the crevices.

When the pH of the crevice solution drops below pH 5, the solubility increases and Al^{+++} becomes the dominant ionic form. Pryor[28] calculated that the lowest possible pH in the system aluminum-water was pH 2.8. The lowest value found in this work, pH 3.8, is thus well above the calculated minimum. The actual steady state value is established as a result of the balance between acidification by hydrolysis, interdiffusion between the crevice solution and the bulk, and the effect of cathodic reactions in the crevice.

The concentration of aluminum ions at pH 3.8 was about three times higher than the values calculated from the solubility product of amorphous aluminum hydroxide as given by Pourbaix,[27]

$$\log (Al^{+++})(OH^-)_3 = -32.34 \tag{4}$$

However, values as high as -31.6 can be found in the literature.[28] The experimental values of aluminum

concentration in the crevice at pH 3.8 would indicate a solubility product of about 31.8 (see Appendix). However, the effect of chlorides on the solubility may be a major factor.

The proportion of alloying elements in the crevice solution was substantially different than in the alloy (Figures 15, 16, 17). Concentrations of zinc and magnesium were higher in the solution, while copper concentration was very low regardless of the type of alloy. A preferential dissolution of anodic $MgZn_2$ precipitates may account for the higher concentrations of zinc and magnesium in the solution in the initial period.[22] In addition both zinc and magnesium compounds have much higher solubility products than aluminum hydroxide; thus they are more likely to stay in solution after the aluminum hydroxide starts to precipitate, which would account for the still higher relative concentration after the transition. The absence of copper in the solution can be explained by copper plating back at the low electrode potentials of the aluminum alloys.

CHAPTER VI

CONCLUSIONS

1. Corrosion of Al-Mg-Zn alloys with various amounts of copper in a sodium chloride solution increased with increasing copper content.

2. The presence of a crevice resulted in an increase in the corrosion rate inside the occluded cell. Under the experimental conditions used in this work the increase was relatively small and insensitive to differences in copper content.

3. The corrosion of the surfaces exposed to the bulk solution was in the form of both general corrosion and pitting. Corrosion in the crevice was in the form of general corrosion, pitting, and selective attack on the grain boundaries.

4. The onset of crevice corrosion was associated with acidification of the solution in the crevice and an increase in chloride ion concentration. The lowest pH in the crevice was 3.8 regardless of the alloy.

5. Results of polarization measurements have shown that the changes in the solution chemistry cause a substantial change in corrosion conditions, all alloys becoming active in the crevice.

6. The proportion of alloying elements in the crevice solutions was different than that in the alloys. The relative amounts of Mg and Zn were higher than in the alloys while the amount of Cu was very low.

7. Observations were in general agreement with the Fontana and Greene Model of crevice corrosion. Quantitative data were close to the results of calculations based on thermodynamical data.

CHAPTER VII

RECOMMENDATIONS

1. The present study was made on alloys aged to near peak hardness conditions. Further information can be obtained by examining the crevice corrosion processes and crevice solution chemistry as a function of heat treatment and microstructure.

2. Further development of the techniques of sampling and analysis would make available more precise data on the solution chemistry for comparison with thermodynamical calculations.

3. This study was made with one geometry of the corrosion cell; experiments with other types of geometry would provide additional information on the kinetics of crevice corrosion.

4. An extension of the present study to an investigation of the localized corrosion conditions existing in microcells, especially at grain boundaries, would be valuable for the understanding of intergranular corrosion and stress corrosion cracking of aluminum alloys.

APPENDIX

Calculation of aluminum concentration in the crevice solution after one hour exposure.

Alloy 76 (Al-Mg-Zn)

Measured: pH 7.6

$$(Al) = 80 \text{ ppm} = 2.96 \times 10^{-3} \text{ M}$$

Calculated from Pourbaix:[27]

$$\log (Al^{+++}) = 9.66 - 3pH = -13.14$$
$$(Al^{+++}) = 7.24 \times 10^{-14} \text{ M}$$
$$\log (AlO_2^{-}) = -10.64 + pH = -3.04$$
$$(AlO_2^{-}) = 9.12 \times 10^{-4} \text{ M}$$

The measured concentration was 3.2 times higher than the calculated value.

Alloy 77 (Al-Mg-Zn-Cu)

Measured: pH 6.7

$$(Al) = 120 \text{ ppm} = 4.4 \times 10^{-2} \text{ M}$$

Calculated:

$$\log(Al^{+++}) = -10.44; \quad (Al^{+++}) = 3.63 \times 10^{-11} \text{ M}$$
$$\log (AlO_2^{-}) + 3.94; \quad (AlO_2^{-}) = 1.14 \times 10^{-4} \text{ M}$$

The measured concentration was 38.9 times higher than the calculated value.

Alloy 7050 (Al-Mg-Zn-Cu)

Measured: pH 7.1

$$(Al) = 90 \text{ ppm} - 3.3 \times 10^{-3} \text{ M}$$

Calculated:

$$\log (Al^{+++}) = -11.64; \quad (Al^{+++}) = 2.2 \times 10^{-12} \text{ M}$$

$$\log (AlO_2^-) = -3.54; \quad (AlO_2^-) = 2.8 \times 10^{-4} \text{ M}$$

The measured concentration was 11.9 times higher than the calculated value.

All Alloys After 100 Hours of Exposure

Measured pH: 3.8 (all alloys)

Measured (Al) concentration:

Alloy 76:   1550 ppm = 5.7×10^{-2} M

Alloy 77:   1650 ppm = 6.1×10^{-2} M

Alloy 7050: 1600 ppm = 5.9×10^{-2} M

Calculations for pH 3.8:

$$\log (Al^{+++}) = 9.66 - 3pH = 1.74$$

$$(Al^{+++}) = 1.8 \times 10^{-2} \text{ M}$$

The measured aluminum ion concentrations were 3.1, 3.4, and 3.3 times higher than the calculated values for alloys 76, 77, and 7050.

Calculation of the Solubility Product

From Pourbaix:[27]

$$\log (Al^{+++})(OH^-)_3 = \text{solubility product}$$

Experimental values:

$$Al^{+++} = 6.1 \times 10^{-2} \text{ (alloy 7050)}$$

$$\log (Al^{+++}) = -1.2$$

$$pH = 3.8; \log (OH^-) = -10.2$$

Substituting directly into Purbaix's equation;

$$\log (Al^{+++})(OH^-) = -31.8$$

BIBLIOGRAPHY

1. C. A. Kesler, "Materials Science in Engineering," (Charles E. Merrill Publishing Co., Columbus, Ohio, 1968).

2. A. G. Guy, "Elements of Physical Metallurgy," (Addison-Wesley Publishing Co., Inc., Reading, Mass, 1960).

3. A. G. Guy, "Physical Metallurgy for Engineers," (Addison-Wesley Publishing Co., Inc., Reading, Mass., 1962).

4. H. P. Goddard, W. P. Jepson, M. R. Bothwell, and R. L. Kane, "The Corrosion of Light Metals," (John Wiley and Sons, Inc., New York, 1967).

5. K. J. Pasco, "An Introduction to Properties of Engineering Materials," (Intrascience Publishers, Inc., New York, 1963).

6. M. Henthorne, "Fundamentals of Corrosion," (Carpenter Technology Corp.).

7. W. H. Ailor, "Aluminum Alloys after Five Years in Sea Water," ASTM 445, (1969).

8. I. L. Rosenfeld and I. K. Marshakov, Zhurnal Fizicheskoi Khimii, ZORKA, 31, (1957).

9. W. D. France, Crevice Corrosion of Metals, STP 561, Philadelphia, Pa., (1972).

10. R. J. McKay, Transaction Electrochemical Socient, TESOA, 41, (1922).

11. U. R. Evans, "An Introduction to Metallic Corrosion," (Edward Arnold, London, 1963).

12. I. L. Rosenfeld and I. K. Marshakov, Mechanisms of Crevice Corrosion, 2, 115, (1964).

13. M. G. Fontana and N. D. Greene, "Corrosion Engineering," (McGraw-Hill, New York, 1967).

14. G. L. Shafer, J. R. Gabriel, and P. K. Foster, On the Role of the Oxygen Concentration Cell in Crevice Corrosion and Pitting, Journal of the Electrochemical Society, 12, 1002, (1960).

15. I. L. Rosenfeld, Review: Crevice Corrosion, "Localized Corrosion," NACE, 373.

16. J. Bryan, The Causes of Localized Character of Corrosion on Aluminum, Society Chemical Industry, 69, 169, (1950).

17. M. G. Fontana and R. W. Staehle, "Advances in Corrosion Science and Technology."

18. C. T. Fujii, A Review: Macro-cells for the Study of Solution Chemistry and Electrochemistry in Localized Corrosion, "Localized Corrosion," NACE, 144.

19. H. Leidheiser and R. Kissinger, Chemical Analysis of the Liquid within a Propagating Stress Corrosion Crack in 70-30 Brass in Concentrated Ammonium Hydroxide, Corrosion, 28, 218, (1972).

20. M. Marek, and R. F. Hochman, Stress Corrosion Cracking of Austenitic Stainless Steel, Corrosion, 26, 5, (1970).

21. G. Sandoz, C. T. Fujii, and B. F. Brown, Solution Chemistry Within Stress Corrosion Cracks in Alloy Steels, Corrosion Science, 10, 839, (1970).

22. M. Marek, J. G. Rinker, and R. F. Hochman, Solution Chemistry in Crevices and Stress Corrosion Cracks, International Conference on Metallic Corrosion, Sydney, Dec. 1975.

23. B. F. Brown, C. T. Fujii, and E. P. Dahlberg, Methods for Studying Solution Chemistry with Stress Corrosion Cracks, Journal of the Electrochemical Society, 116, 218.

24. A. J. Sedriks, J. A. S. Green, and D. L. Novak, Corrosion Processes and Solution Chemistry within Stress Corrosion Cracks in Aluminum Alloys, "Localized Corrosion," NACE, 556.

25. L. Green, unpublished research.

26. T. Sanders, Thesis, Georgia Tech, 1975.

27. M. Pourbaix, Atlas of Electrochemical Equilibria in Aqueous Solutions, NACE--CEBELCOR (1974).

28. M. J. Pryor, The Influence of the Defect Structure of Aluminum Oxide Films on the Pitting of Aluminum in Chloride Solutions, "Localized Corrosion," NACE, 2.